Published in final edited form as:

Cell Rep. 2020 September 01; 32(9): 108085. doi:10.1016/j.celrep.2020.108085.

CD49a Regulates Cutaneous Resident Memory CD8+ T Cell Persistence and Response

Shannon K. Bromley[1,4,*], **Hasan Akbaba**[1,2], **Vinidhra Mani**[1,3], **Rut Mora-Buch**[1], **Alexandra Y. Chasse**[1], **Andrea Sama**[1], **Andrew D. Luster**[1]

[1]Center for Immunology and Inflammatory Diseases, Division of Rheumatology, Allergy and Immunology, Massachusetts General Hospital, Harvard Medical School, Boston, MA, USA

[2]Department of Pharmaceutical Biotechnology Faculty of Pharmacy, Ege University, 35100, Bornova, Izmir, Turkey

[3]Immunology Graduate Program, Harvard Medical School, Boston, MA, USA

[4]Lead Contact

SUMMARY

$CD8^+$ tissue-resident memory T cells (T_{RM}) persist at sites of previous infection, where they provide rapid local protection against pathogen challenge. $CD8^+$ T_{RM} expressing the α1 chain (CD49a) of integrin VLA-1 have been identified within sites of resolved skin infection and in vitiligo lesions. We demonstrate that CD49a is expressed early following T cell activation *in vivo,* and TGF-β and IL-12 induce CD49a expression by $CD8^+$ T cells *in vitro.* Despite this rapid expression, CD49a is not required for the generation of a primary $CD8^+$ T cell response to cutaneous herpes simplex virus (HSV) infection, migration of $CD8^+$ T cells across the epidermal basement membrane, or positioning of T_{RM} within basal epidermis. Rather, CD49a supports $CD8^+$ T_{RM} persistence within skin, regulates epidermal $CD8^+$ T_{RM} dendritic extensions, and increases the frequency of IFN-γ^+ $CD8^+$ T_{RM} following local antigen challenge. Our results suggest that CD49a promotes optimal cutaneous $CD8^+$ T_{RM}-mediated immunity.

Graphical Abstract

*Correspondence: sbromley@mgh.harvard.edu.

AUTHOR CONTRIBUTIONS

S.K.B., H.A., V.M., R.M.-B., A.Y.C., and A.S. performed experiments. H.A. and A.Y.C. analyzed and interpreted data. S.K.B. designed experiments, analyzed and interpreted data, and wrote the manuscript. A.D.L. made important conceptual contributions and contributed to writing the manuscript.

SUPPLEMENTAL INFORMATION

Supplemental Information can be found online at https://doi.org/10.1016/j.celrep.2020.108085.

DECLARATION OF INTERESTS

The authors declare no competing interests.

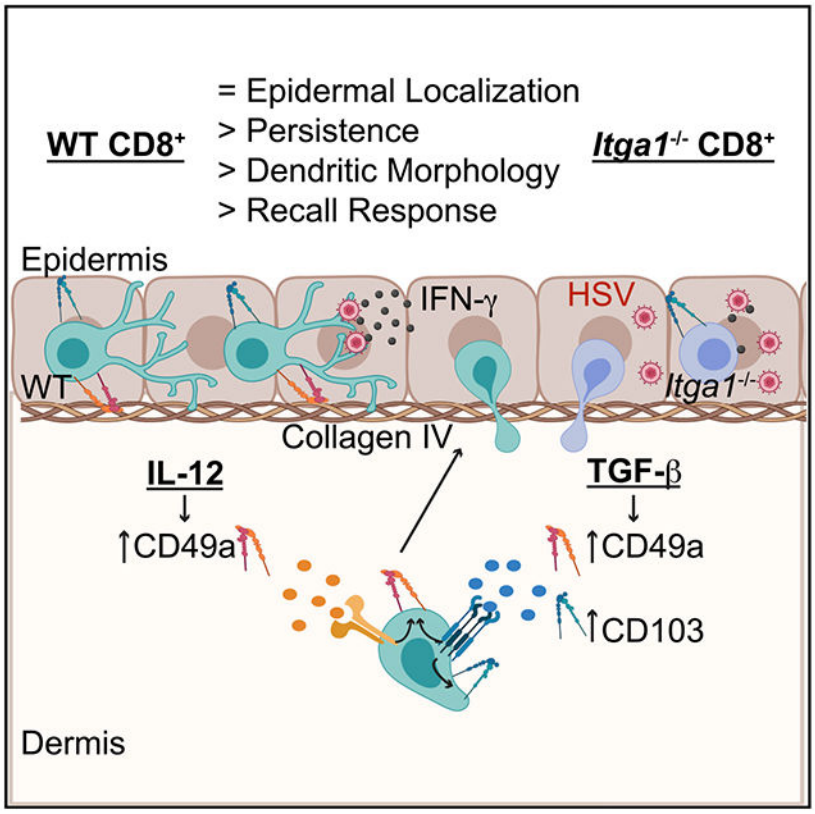

In Brief

Bromley et al. demonstrate that IL-12 or TGF-β can induce CD49a expression by $CD8^+$ T cells. Following herpes simplex virus infection, CD49a is not required for $CD8^+$ T cell entry into or localization within the epidermis. Rather, CD49a promotes skin T_{RM} persistence, dendritic morphology, and optimal response to antigen challenge.

INTRODUCTION

Infection induces the migration of effector T cells into inflamed peripheral tissues. Upon resolution of the immune response, the majority of effectors die by apoptosis. However, a subset of memory T cells persists long-term within peripheral tissues (Gebhardt et al., 2009; Klonowski et al., 2004; Masopust et al., 2010). These tissue-resident memory T cells (T_{RM}) are generated from memory precursor cells within peripheral tissues in response to local cytokine cues (Casey et al., 2012; Mackay et al., 2012) and acquire a phenotype distinct from circulating memory T cells (Mackay et al., 2013, 2016; Masopust et al., 2006; Wakim et al., 2012). Following cutaneous herpes simplex virus (HSV) infection, $CD8^+$ T cells migrate through the dermis and into the epidermis, where they upregulate expression of CD103, the α chain of integrin αEβ7. $CD103^+$ $CD8^+$ T_{RM} persist adjacent to the epidermal basement membrane (Mackay et al., 2013), where they are strategically positioned to provide rapid local memory response against cutaneous pathogen challenge (Gebhardt et al., 2009; Jiang et al., 2012; Teijaro et al., 2011; Wu et al., 2014).

Several tissue-resident cell types, including $CD8^+$ T_{RM}, also express the adhesion receptor CD49a (Chapman and Topham, 2010; Dadi et al., 2016; Gebhardt et al., 2009; Oja et al., 2018; Peng et al., 2013; Ray et al., 2004). Integrin subunit alpha 1 (*Itga1*) encodes CD49a, the α chain of the α1β1 integrin very late antigen-1 (VLA-1). VLA-1 was named on the basis of the finding that it is expressed on long-term activated T cells *in vitro* (Hemler et al., 1985). *In vivo,* CD49a has been detected on T_{RM} recovered from tissues, including skin, late following resolution of infection (Gebhardt et al., 2009; Mackay et al., 2016; Ray et al., 2004). Moreover, a recent study determined that CD49a expression identifies human cutaneous $CD8^+$ T_{RM} poised for IFN-γ secretion and cytotoxic function (Cheuk et al., 2017). Although these expression analyses are suggestive of a possible role for CD49a in the regulation of cutaneous $CD8^+$ T_{RM} immune response, the mechanisms that regulate $CD8^+$ T_{RM} CD49a expression and its role in promoting $CD8^+$ T_{RM}-mediated immunity *in vivo* are incompletely defined.

CD49a can be expressed rapidly by T cells during inflammation (Andreasen et al., 2003; Haddadi et al., 2017), and so VLA-1 may regulate T_{RM} at multiple stages: T_{RM} precursor recruitment, T_{RM} formation, persistence, and response. VLA-1 binds collagen I, collagen IV, and laminin, major components of the extracellular matrix (Gardner, 2014), and VLA-1 plays an essential role in leukocyte migration within skin in several mouse models of cutaneous inflammation (Andreasen et al., 2003; de Fougerolles et al., 2000). Additionally, a critical role for VLA-1 in disease development was found using a xenotransplantation model of psoriasis. Collagen IV and laminin are components of the epidermal basement membrane, and T cells required VLA-1 for entry into the epidermis and induction of the psoriatic phenotype (Conrad et al., 2007). Given that $CD8^+$ T cell epidermal entry is required for $CD8^+$ T_{RM} CD103 expression and long-term persistence following HSV infection (Mackay et al., 2013), we hypothesized that VLA-1 might be essential for T cell entry into the epidermis for $CD103^+$ T_{RM} formation.

Imaging studies demonstrate that T_{RM} migrate slowly within the skin, preferentially maintaining contact with the epidermal basement membrane. These T cells exhibit a dendritic morphology, extending dendrites laterally along the basement membrane, which is predicted to facilitate their patrol of skin for cognate antigen (Ariotti et al., 2012; Zaid et al., 2014). Within hours after local cognate antigen challenge, $CD8^+$ T_{RM} secrete cytokines that activate innate immune cells and induce expression of chemokines, resulting in recruitment of circulating memory T cells and amplification of the memory response (Ariotti et al., 2014; Schenkel et al., 2013, 2014). CD49a expression has been identified on T cells that are enriched for IFN-γ secretion, suggesting that CD49a may identify T cells with distinct effector function (Cheuk et al., 2017; Goldstein et al., 2003). However, whether CD49a is required for the differentiation of IFN-γ-secreting T_{RM} or their response to local antigen challenge *in vivo* is unknown.

Here, using a mouse model of cutaneous HSV infection, we examined the requirement for CD49a in the formation, localization, persistence, and function of cutaneous $CD8^+$ T_{RM}. We demonstrated that CD49a was expressed early following T cell activation and could be detected on circulating HSV-specific $CD8^+$ T cells before their entry into HSV-infected skin. Unlike CD103, CD49a was induced not only by TGF-β but also by IL-12. Nonetheless,

despite this early CD49a expression by wild-type (WT) $CD8^+$ T cells, *Itga1*$^{-/-}$ $CD8^+$ T cells differentiated and initially entered into infected skin comparably with WT $CD8^+$ T cells. Moreover, *Itga1*$^{-/-}$ T cells were able to migrate through the dermis, across the epidermal basement membrane, and into the epidermis, where they expressed CD103 and effectively cleared replicating virus. However, fewer *Itga1*$^{-/-}$ $CD8^+$ T_{RM} than WT T_{RM} were recovered from skin 35 days following HSV infection. Imaging of *Itga1*$^{-/-}$ $CD8^+$ skin T_{RM} demonstrated that they were less dendritic than WT $CD8^+$ T_{RM}, and this correlated with a decreased memory IFN-γ response following cognate antigen challenge. Thus, we demonstrate that CD49a was not required for the generation of a primary $CD8^+$ T cell response to cutaneous HSV infection or for the formation of $CD8^+$ T_{RM}. However, CD49a regulated $CD8^+$ T_{RM} persistence and effector function, promoting robust response to local antigen challenge.

RESULTS

CD49a Is Expressed Early on $CD8^+$ T Cells following HSV Infection

To determine the requirements for CD49a in cutaneous $CD8^+$ T_{RM} formation, we used a mouse zosteriform model of HSV infection (Goel et al., 2002; van Lint et al., 2004). We first analyzed CD49a expression by endogenous $CD8^+$ T cells specific for the HSV gB determinant. Mice were infected with HSV-1 KOS (Colgrove et al., 2016) by skin scarification, and after 9–30 days, cells recovered from the skin infection site, contralateral skin, spleen, and draining brachial lymph node (LN) were stained with H2-K^b MHC class I tetramers containing the immunodominant gB(498–505) peptide epitope and with antibody directed against CD49a. In agreement with previous studies (Gebhardt et al., 2009), we found that CD49a was expressed on >95% of cutaneous memory HSV-specific $CD8^+$ T cells recovered from the primary infection site 30 days post-infection (Figure 1A). At this memory time point, CD49a expression was enriched on cutaneous memory H-2K^b-HSV/gB$^+$ $CD8^+$ $CD44^{hi}$ T cells compared with those recovered from the spleen or draining LNs. We also examined CD49a expression by HSV-specific $CD8^+$ T cells recovered from contralateral skin 30 days post-infection. Although most HSV-specific $CD8^+$ T cells isolated from contralateral skin also expressed CD49a at this memory time point (Figure 1A), many more HSV-specific $CD8^+$ T cells were recovered from the ipsilateral flank skin compared with the uninvolved contralateral skin (Figure S1).

The T_{RM} adhesion receptor CD103 is expressed on cutaneous $CD8^+$ T cells late following HSV infection, and deletion of *Itgae* (encoding CD103) prevents the persistence of epidermal $CD8^+$ T_{RM} (Mackay et al., 2013). To determine whether CD49a, like CD103, is expressed only late following infection, we examined the kinetics of CD49a expression. Although the majority of $CD8^+$ T cells recovered from the initial skin infection site at a memory time point co-expressed CD49a and CD103, CD49a expression preceded CD103 on cutaneous $CD8^+$ T cells (Figures 1B and 1C). Greater than 70% of $CD8^+$ T cells within the skin expressed CD49a at the peak of the response (day 9 [d9]) post-HSV infection. In contrast, cutaneous $CD8^+$ T cells lacked CD103 expression at this early time point. These results suggest that although CD103 expression is acquired only after $CD8^+$ T cell entry into the skin, CD49a expression by $CD8^+$ T cells may be induced in the lymphoid tissues early

after activation, and before their migration into non-lymphoid tissues. Indeed, analysis of HSV-specific $CD8^+$ T cells recovered from secondary lymphoid tissues and the circulation demonstrated they expressed CD49a, but not CD103 early (d7) following infection (Figure 1D).

CD49a and CD103 Expression May Be Differentially Regulated

Given our findings that CD49a is induced earlier on cutaneous $CD8^+$ T cells than CD103, and that CD49a is induced on $CD8^+$ T cells within lymphoid tissues while CD103 is not, we next generated *in vitro* cultures to examine whether CD49a and CD103 are differentially regulated by cytokines. Previous studies have demonstrated that TGF-β drives CD103 and CD49a expression by $CD8^+$ T cells *in vivo* (Casey et al., 2012; Mackay et al., 2013; Wang et al., 2004; Zhang and Bevan, 2013). Additionally, *in vitro* culture of early $CD8^+$ T cell effectors with TGF-β induces their expression of CD103 (Casey et al., 2012). In agreement with these data, we found that culture of d5 *in vitro*-activated $CD8^+$ T cells with TGF-β induced their expression of both CD49a and CD103. We then tested whether culture with various other cytokines could induce $CD8^+$ T_{RM} receptor expression. Although most cytokines tested had no effect, we found that IL-12 alone induced expression of CD49a, but not CD103. Furthermore, addition of IL-12 along with TGF-β to $CD8^+$ T cell cultures inhibited TGF-β-induced CD103 expression but did not prevent expression of CD49a (Figures 2A and 2B).

Differentiation of T_{RM} is thought to be regulated by the local tissue microenvironment. $KLRG1^-$ $CD8^+$ early effector T cells adoptively transferred directly into the skin upregulate expression of the T_{RM} adhesion receptor CD103 *in situ* (Mackay et al., 2013). To determine whether the local microenvironment can also induce expression of CD49a by cutaneous $CD8^+$ T cells, we adoptively transferred d5 *in vitro*-activated $CD8^+$ T cells either intradermally or intravenously into congenic recipient mice. After 9 days, we recovered the adoptively transferred $CD8^+$ T cells from the skin and spleen, respectively, and analyzed their expression of CD49a and CD103. In agreement with published literature, $CD8^+$ T cells upregulated CD103 expression following their direct intradermal transfer (Mackay et al., 2013). In contrast, $CD8^+$ T cells recovered from secondary lymphoid tissues following intravenous transfer lacked CD103 expression. In parallel, we found that $CD8^+$ T cells recovered from skin following their direct intradermal transfer were enriched for CD49a expression (Figures 2C and 2D). Our experiment did not exclude the possibility that $CD8^+$ T cells exited skin, recirculated through lymphoid tissues, and expressed CD49a before reentering the skin. However, because the geometric mean fluorescence intensity (gMFI) of CD49a staining was higher for $CD8^+$ T cells recovered from skin compared with those recovered from spleen (Figure 2C; Figure S2), our results suggest that the local microenvironment can induce and/or increase CD49a expression by $CD8^+$ T cells after their entry into peripheral tissues.

CD49a Is Not Required for $CD8^+$ T Cell Activation, Tissue Entry, or Viral Clearance

Because CD49a is expressed on a fraction of $CD8^+$ T cells early after HSV infection, we examined whether VLA-1 plays an essential role in initial $CD8^+$ T cell activation or differentiation. Seven days following infection, we isolated the spleen, draining LN, and

initial skin infection site and stained recovered leukocytes with H-2K^b-HSV/gB tetramerto identify endogenous HSV-specific CD8$^+$ T cells and with antibodies directed against the T cell differentiation markers CD44, KLRG1, and CD62L. A similar fraction of WT and *Itga1*$^{-/-}$ H-2K^b-HSV/gB$^+$ CD8$^+$ T cells expressed the T cell activation/memory marker CD44 (Figure 3A). T_{RM} are thought to differentiate from KLRG1$^-$ CD8$^+$ precursor cells (Mackay et al., 2013), and flow cytometric analysis demonstrated a comparable fraction of KLRG1$^-$ H-2K^b-HSV/gB$^+$ CD8$^+$ T cells within secondary lymphoid tissues and skin of WT and *Itga1*$^{-/-}$ mice following HSV infection (Figure 3A). Most WT and *Itga1*$^{-/-}$ H-2K^b-HSV/gB$^+$ CD8$^+$ T cells recovered from skin had downregulated expression of the lymphoid tissue homing receptor CD62L (Figure 3A).

Previous studies have correlated T cell granzyme B expression and IFN-γ secretion with T cell CD49a expression (Cheuk et al., 2017; Goldstein et al., 2003). Given this link between CD49a expression and CD8$^+$ T cell effector function, we examined whether *Itga1* deficiency impaired the differentiation of CD8$^+$ T cells following HSV infection. A similar fraction of CD8$^+$ T cells isolated from both the spleen and initial skin infection site of WT and *Itga1*$^{-/-}$ mice expressed granzyme B (Figure 3B, left panel), and there was no difference in mean fluorescence intensity (gMFI) of granzyme B staining (Figure 3B, right panel). Similarly, a comparable fraction of recovered WT and *Itga1*$^{-/-}$ CD8$^+$ T cells generated IFN-γ following *in vitro* re-stimulation (Figure 3C, left panel), and there was no significant difference in IFN-γ gMFI (Figure 3C, right panel). Together, these results suggest that WT and *Itga1*$^{-/-}$ CD8$^+$ T cells differentiated comparably. Additionally, *Itga1*$^{-/-}$ CD8$^+$ T cells appeared to expand normally; equivalent numbers of HSV-specific CD8$^+$ T cells were recovered from the spleen and draining LNs of WT and *Itga1*$^{-/-}$ mice 7 days post-infection (Figure 3D). Notably, *Itga1*$^{-/-}$ HSV-specific CD8$^+$ T cells were able to initially enter into the skin, as we recovered H-2K^b-HSV/gB$^+$ CD8$^+$ T cells from the initial skin infection site of both WT and *Itga1*$^{-/-}$ mice 7 days post-infection (Figure 3D).

Replicating HSV can be cleared from the skin at the primary site of infection in the absence of CD8$^+$ T cells (Manickan and Rouse, 1995; Nash et al., 1987). Nonetheless, as CD49a is expressed on multiple cells types, we next determined whether lack of CD49a affects the ability of mice to clear replicating HSV from the skin. WT and *Itga1*$^{-/-}$ mice were infected with HSV-1 by skin scarification. Four, 7, 9, and 14 days post-infection, a 1 cm^2 piece of skin at the initial skin infection site was isolated, and plaque assays were performed on tissue homogenates. Control of cutaneous infection was similar; replicating virus yield from the skin of WT and *Itga1*$^{-/-}$ mice was comparable at each time point tested (Figure 3E). These data demonstrate that WT and *Itga1*$^{-/-}$ CD8$^+$ T cells are activated, differentiate, and migrate comparably into skin to control HSV infection.

CD8$^+$ T Cell Epidermal Entry Is CD49a Independent

CD8$^+$ T cell entry into the epidermis is a critical step in the formation of cutaneous CD103$^+$ T_{RM} following HSV infection (Mackay et al., 2013). CD49a ligands are components of the epidermal basement membrane, so T cell migration from the dermis into the epidermis might depend on CD49a-ligand interactions. To determine whether CD49a expression by HSV-specific CD8$^+$ T cells is required for their entry into the epidermis following HSV

infection, the skin at the initial infection site of WT and *Itga1*$^{-/-}$ mice was isolated 14 days post-infection, a time point when most cutaneous WT H-2K^{b}-HSV/gB^{+} CD8^{+} T cells express CD49a, and ~50% express CD103 (Figure 1B). Then, epidermis was separated from dermis, and numbers of recovered epidermal and dermal H-2K^{b}-HSV/gB^{+} CD8^{+} T cells were quantitated. We identified similar numbers of H-2K^{b}-HSV/gB^{+} CD8^{+} T cells within the epidermis of WT and *Itga1*$^{-/-}$ mice (Figure 3F), suggesting that CD8^{+} T cell epidermal entry in this mouse model of HSV infection is CD49a independent.

Fewer Itga1$^{-/-}$ Than WT CD8^{+} T_{RM} Persist in Previously Infected Skin

Although we found that WT and *Itga1*$^{-/-}$ CD8^{+} T cells were able to initially enter into skin and migrate into the epidermis, we hypothesized that CD49a might promote the formation and maintenance of CD8^{+} memory T cells within the skin. To determine whether CD49a promotes T_{RM} persistence within skin, we isolated the spleen and the skin at the initial infection site from WT and *Itga1*$^{-/-}$ mice 35 days post-HSV infection. Similar numbers of H-2K^{b}-HSV/gB CD8^{+} CD44^{hi} T cells were recovered from the spleen of *Itga1*$^{-/-}$ and WT mice. However, fewer H-2K^{b}-HSV/gB CD8^{+} CD44^{hi} T cells were recovered from the skin of *Itga1*$^{-/-}$ mice compared with WT mice, suggesting that CD49a expression facilitates cutaneous CD8^{+} T_{RM} formation and/or persistence following HSV infection (Figure 4A). At this memory time point, most *Itga1*$^{-/-}$-HSV-gB/K^{b} CD8^{+} CD44^{hi} T cells recovered from the skin expressed CD103, indicating that CD49a is not required for subsequent differentiation to a CD8^{+} CD103^{+} T_{RM} phenotype (Figure 4B). However, CD49a is advantageous for the persistence of CD8^{+} T_{RM} within this barrier tissue.

In addition to CD8^{+} T cells, other immune cells, including CD4^{+} T cells and tissue-resident natural killer (NK) cells, express CD49a. To determine whether CD8^{+} T cells require CD49a expression for their persistence within skin, we adoptively transferred naive WT OT-I CD8^{+} T cells (which have transgenic expression of a T cell receptor [TCR] specific for ovalbumin) or *Itga1*$^{-/-}$ CD8^{+} OT-I T cells intravenously into congenic recipient WT mice. The next day, recipient mice were infected with recombinant HSV expressing ovalbumin (HSV-OVA). After 35 days, the spleen and skin at the initial infection site were isolated, and recovered CD8^{+} OT-I CD44^{hi} T cells were quantitated. Although similar numbers of WT and *Itga1*$^{-/-}$ CD44^{hi} CD8^{+} OT-I T cells were recovered from spleen, fewer *Itga1*$^{-/-}$ than WT CD44^{hi} CD8^{+} OT-I T_{RM} were recovered from previously infected skin (Figure 4C). Again, at this memory time point, most *Itga1*$^{-/-}$ CD44^{hi} OT-I T cells recovered from the skin expressed CD103, indicating that CD49a is not required for subsequent differentiation to a CD8^{+} CD103^{+} T_{RM} phenotype (Figure 4D). These data suggest that CD49a expression by CD8^{+} T_{RM} promotes their persistence within the epidermis.

CD8^{+} T_{RM} contribute to protection from HSV challenge (Gebhardt et al., 2009; Park et al., 2018). Given that CD49a expression was important for CD8^{+} T_{RM} persistence within skin, we next compared viral clearance by WT and *Itga1*$^{-/-}$ CD8^{+} T_{RM}. To induce cutaneous CD8^{+} T_{RM}, WT or *Itga1*$^{-/-}$ CD8^{+} T cells were adoptively transferred into recipient mice followed by injection with OVA-DNA in the flank skin (Mani et al., 2019). We hypothesized that mice harboring *Itga1*$^{-/-}$ CD8^{+} OT-I T_{RM} within flank skin would have higher viral titers than mice containing WT OT-I T_{RM} following challenge with HSV-OVA. In fact, 4 days

post-virus challenge, HSV titers in the skin were ~2-fold higher in mice harboring *Itga1*$^{-/-}$ CD8^{+} OT-I T_{RM} (Figure 4E), suggesting that reduced numbers of *Itga1*$^{-/-}$ CD8^{+} T_{RM} in the skin may contribute to impaired viral clearance.

CD49a Expression Contributes to Epidermal T_{RM} Morphology

To better understand the role for CD49a in T_{RM} function within the skin, we first examined the effect of *Itga1* deficiency on T_{RM} positioning within the skin. Quantitation of WT and *Itga1*$^{-/-}$ CD8^{+} OT-I T_{RM} in confocal images again suggested fewer *Itga1*$^{-/-}$ than WT CD8^{+} OT-I T_{RM} were resident within the skin (Figures 5A and 5B, left panel). However, both WT and *Itga1*$^{-/-}$ CD8^{+} OT-I T_{RM} lodged within the epidermis, adjacent to the dermal-epidermal border (Figures 5A and 5B, middle panel). Additionally, similar fractions of WT and *Itga1*$^{-/-}$ CD8^{+} OT-I T_{RM} were detected in interfollicular epithelium and in hair follicle epithelium (Figure 5B, right panel), suggesting that *Itga1*$^{-/-}$ CD8^{+} T_{RM} localized normally within the epidermis following HSV infection.

Previous studies proposed that following HSV-1 infection, epithelial CD8^{+} T_{RM} replace γδ T cells (Zaid et al., 2014), perhaps by competing for space and/or survival signals. Because we recovered decreased numbers of CD8^{+} OT-I T_{RM} from the skin of *Itga1*$^{-/-}$ compared with WT mice, we next asked whether increased numbers of γδ T or CD8^{+} T cells persisted in the skin of *Itga1*$^{-/-}$ mice. γδ T cells were largely excluded from areas closest to the initial HSV infection site in both WT and *Itga1*$^{-/-}$ mice, where densities of CD8^{+} OT-I T_{RM} were highest (Figure 5A). However, γδ T cells were readily observed in areas more distal to the site of initial infection (Figure S3), and the total numbers of γδ T cells within a 1 cm^2 area of skin surrounding the site of initial HSV infection did not significantly differ between WT and *Itga1*$^{-/-}$ mice (Figure 5C, left panel). In contrast, numbers of epithelial CD8^{+} T cells were decreased in *Itga1*$^{-/-}$ mice compared with WT mice (Figure 5C, right panel). These results suggest that although CD49a is not required for the persistence of γδ T cells, γδ T cells do not replace *Itga1*$^{-/-}$ CD8^{+} T_{RM} within the epithelium.

Previous imaging studies demonstrated that epidermal CD8^{+} T_{RM} migrate slowly within the epidermis but continuously extend and retract cellular processes (Ariotti et al., 2012; Zaid et al., 2014). To determine whether CD49a regulates epidermal CD8^{+} T_{RM} interaction with the extracellular matrix, >30 days post-HSV infection, whole mounts of flank skin from WT and *Itga1*$^{-/-}$ mice were stained with antibodies directed against CD8β. Z stack confocal images were acquired, and epidermis and dermis were distinguished by differences in autofluorescence (Figure S4). Confocal image analysis demonstrated that epidermal WT CD8^{+} T cells were elongated, with numerous, often multi-branched cell processes extending in multiple directions (Ariotti et al., 2012; Zaid et al., 2014; Figure 5D). Epidermal *Itga1*$^{-/-}$ CD8^{+} T cells were also spread, but generally appeared less elongated and less dendritic than WT CD8^{+} T cells (Figure 5D). Cell circularity measurements of confocal maximum intensity projections, where the circularity of a perfectly round cell measures 1.0, confirmed that *Itga1*$^{-/-}$ CD8^{+} T cells were on average more circular than WT CD8^{+} T cells (Figure 5E). These data suggest that CD49a regulates interactions of epidermal CD8^{+} T_{RM} with the tissue, influencing their formation of dendritic projections.

CD49a Regulates CD8$^+$ T_{RM} Response to Antigen Challenge

CD8$^+$ T_{RM} extension of dendritic protrusions is proposed to facilitate their interaction with cognate antigen (Ariotti et al., 2012). Given our finding that *Itga1*$^{-/-}$ CD8$^+$ T_{RM} appeared less dendritic than WT CD8$^+$ T_{RM}, we hypothesized that *Itga1* deficiency might impair the ability of cells to respond to local antigen challenge. Previous studies have demonstrated that following antigen challenge, CD8$^+$ T_{RM} secrete IFN-γ, which activates innate cells and induces expression of chemokines and adhesion receptors, facilitating the recruitment of additional cells into the tissue for pathogen control (Ariotti et al., 2014; Schenkel et al., 2013, 2014). Therefore, we examined IFN-γ secretion as a readout for WT and *Itga1*$^{-/-}$ CD8$^+$ T_{RM} response to cognate antigen challenge. First, WT and *Itga1*$^{-/-}$ mice were infected with HSV-KOS. Then, in order to ensure that we studied local CD8$^+$ T_{RM} response to antigen challenge, 30 days post-infection, mice were injected intraperitoneally (i.p.) with anti-CD8 antibody to deplete circulating CD8$^+$ T cells. After 4 days, mice were challenged by intradermal injection with 3 μg HSV gB(498–505) cognate peptide or with 3 μg OVA(257–264) control peptide at the initial infection site. Ten hours later, the skin injection site was isolated for gene expression analysis of *Ifng* and the IFN-γ-induced chemokines *Cxcl9* and *Cxcl10*. qRT-PCR analysis revealed that *Itga1*$^{-/-}$ mice expressed significantly less *Ifng* and *Cxcl9* than WT mice following challenge with HSV gB(498–505) (Figure 6A). These results suggest that the total expression of *Ifng* and IFN-γ-induced chemokines is decreased in the skin of *Itga1*$^{-/-}$ mice following cognate antigen challenge.

Previous studies demonstrated that culturing CD49a$^+$ CD8$^+$ T_{RM} on collagen-coated wells during activation increases the frequency of IFN-γ-secreting CD8$^+$ T cells compared with CD49a$^+$ CD8$^+$ T_{RM} activated in uncoated wells (Cheuk et al., 2017). Therefore, we examined whether the increased *Ifng* expression observed in the skin of WT compared with *Itga1*$^{-/-}$ mice following antigen challenge (Figure 6A) is simply due to the increased numbers of WT T_{RM} versus *Itga1*$^{-/-}$ T_{RM} present in the skin at a memory time point (Figures 4A and 4C), or whether CD49a increases the frequency of IFN-γ-secreting CD8$^+$ T_{RM} following cognate antigen challenge *in vivo.* WT or *Itga1*$^{-/-}$ CD8$^+$ OT-I T cells were transferred into recipient congenic mice, which were then infected with HSV-OVA. Again, after 30 days, mice were injected i.p. with anti-CD8α antibody to deplete circulating CD8$^+$ T cells. Four days later, mice were challenged by intradermal injection of cognate OVA peptide. After 10 h, mice were injected intravenously (i.v.) with brefeldin A in order to prevent cytokine secretion and allow detection of CD8$^+$ T cells actively producing IFN-γ *in vivo*. Six hours later, the skin injection site was isolated, and the fractions of WT and *Itga1*$^{-/-}$ CD8$^+$ OT-I T cells secreting IFN-γ were quantitated by flow cytometry. The frequency of IFN-γ$^+$ *Itga1*$^{-/-}$ OT-I T_{RM} was reduced by ~50% compared with IFN-γ$^+$ WT OT-I T_{RM} (Figure 6B). These data demonstrate that *in vivo*, CD49a-ligand interactions increase the frequency of IFN-γ$^+$ WT CD8$^+$ T_{RM} compared with IFN-γ$^+$ *Itga1*$^{-/-}$ CD8$^+$ T_{RM} following local cutaneous antigen challenge.

DISCUSSION

Our results describe the expression and function of the adhesion receptor CD49a in cutaneous CD8$^+$ T_{RM}. *Itga1*$^{-/-}$ CD8$^+$ T cells were initially activated, differentiated, migrated

into HSV-infected skin, and cleared replicating virus comparably with WT $CD8^+$ T cells. Additionally, *Itga1*$^{-/-}$ $CD8^+$ T cells migrated through the dermis and entered into the epidermis, where they expressed CD103. Despite the formation of *Itga1*$^{-/-}$ epidermal $CD8^+$ $CD103^+$ T_{RM}, fewer *Itga1*$^{-/-}$ than WT $CD8^+$ T_{RM} persisted long-term within the skin. Confocal image analysis of whole-mount skin demonstrated that *Itga1*$^{-/-}$ $CD8^+$ T_{RM} were less dendritic than WT $CD8^+$ T_{RM}. Moreover, although *Itga1*$^{-/-}$ $CD8^+$ effector T cells differentiated and secreted IFN-γ upon *ex vivo* stimulation, *Itga1*$^{-/-}$ $CD8^+$ T_{RM} exhibited decreased effector function *in vivo* following cognate antigen challenge. Impaired viral clearance in the memory phase might be caused by both reduced *Itga1*$^{-/-}$ $CD8^+$ T_{RM} persistence as well as effector response. Thus, our study defines a role for CD49a in regulating cutaneous $CD8^+$ T_{RM} persistence and response.

Using a zosteriform model of HSV infection, we demonstrated that CD49a is expressed early following T cell activation and was detected on lymphoid and circulating $CD8^+$ T cells before their entry into HSV-infected skin. TGF-β induces both CD49a and CD103 expression *in vivo* (Casey et al., 2012; Mackay et al., 2013; Wang et al., 2004; Zhang and Bevan, 2013). However, CD49a was induced more rapidly than CD103 on $CD8^+$ T cells following HSV infection, suggesting different molecular regulation of their expression. Our *in vitro* culture studies demonstrated that whereas IL-12 upregulated CD49a expression, it inhibited TGF-β-induced CD103 expression. Previous studies revealed that IL-12 inhibits CD103 expression by $CD8^+$ T cells following Yersinia infection, and $CD103^-$ $CD69^+$ $CD8^+$ T cells localize in clusters in the intestinal lamina propria of infected mice (Bergsbaken et al., 2017). Expression of CD49a by these $CD103^-$ $CD8^+$ T_{RM} was not examined, but IL-12-induced CD49a expression is one possible mechanism contributing to the persistence of $CD103^-$ T_{RM} within tissues. Like *Itga1*$^{-/-}$ $CD8^+$ T_{RM}, *Itgae*$^{-/-}$ T_{RM} also exhibit a defect in their long-term persistence within skin (Mackay et al., 2013). It will be interesting to determine whether dual deficiency in CD49a and CD103 might have a more profound effect on maintenance of cutaneous T_{RM} than deficiency of either individual receptor.

Despite rapid CD49a expression by WT $CD8^+$ T cells following HSV infection, *Itga1*$^{-/-}$ $CD8^+$ T cells were activated, differentiated and initially entered into infected skin comparably with WT T cells. Upon entry into the skin, *Itga1*$^{-/-}$ T cells were able to migrate through the dermis, across the epidermal basement membrane, localize in the basal epidermis, and effectively clear replicating virus. In contrast, in a xenotransplantation model of psoriasis, CD49a blockade prevents the migration of T cells from the dermis into the epidermis (Conrad et al., 2007). The reason for this difference in the requirement for CD49a expression is unclear, but perhaps in the setting of HSV infection, additional adhesion receptors are expressed by $CD8^+$ T cells and/or by the HSV-infected skin that compensate for lack of CD49a expression and allow $CD8^+$ T cell migration into and positioning within the epidermis. Although *Itga1*$^{-/-}$ $CD8^+$ T cells were able to enter into the epidermis, fewer $CD8^+$ memory T cells were recovered from the skin of *Itga1*$^{-/-}$ mice compared with WT mice 35 days post-HSV infection. Nonetheless, within the epidermis, *Itga1*$^{-/-}$ $CD8^+$ T cells expressed CD103, demonstrating that CD49a was not required for $CD8^+$ T_{RM} formation per se, but provided an advantage for T_{RM} persistence. These results parallel a previous study in which numbers of memory $CD8^+$ T cells recovered from the lung late following influenza infection were decreased in *Itga1*$^{-/-}$ mice compared with WT mice, as well as in WT mice

treated with a CD49a-neutralizing antibody (Ray et al., 2004). Our results further demonstrate that the CD49a requirement for cutaneous $CD8^+$ $CD103^+$ T_{RM} formation is T cell intrinsic. Fewer adoptively transferred *Itga1*$^{-/-}$ than WT OT-I $CD8^+$ $CD103^+$ T cells persisted within the skin following HSV-OVA infection. CD49a is expressed by multiple tissue-resident cell types, including, for example, NKT cells (Mackay et al., 2016) and tissue-resident NK cells (Mackay et al., 2016; Peng et al., 2013). Whether CD49a also regulates the persistence of these innate lymphoid cells within tissues is unknown.

Both their tight confinement within the epidermis and their interaction with the epidermal environment may regulate $CD8^+$ T_{RM} dendritic morphology. Indeed, previous imaging studies measured differences in dendrite projection angles between epidermal $CD8^+$ T_{RM} and γδ T cells, suggesting that cell-specific interactions with their surroundings may regulate cell dendrite extensions (Ariotti et al., 2012; Zaid et al., 2014). Our immunofluorescence confocal imaging demonstrated that *Itga1*$^{-/-}$ $CD8^+$ T_{RM} were more circular than WT $CD8^+$ T_{RM} within the skin. Although neither WT nor *Itga1*$^{-/-}$ $CD8^+$ T_{RM} were entirely rounded, WT $CD8^+$ T cells appeared more elongated, with numerous dendritic extensions. However, the requirements for adhesion receptors in regulating T_{RM} behavior might differ depending on the experimental system and/or tissue examined. Differences in integrin and integrin ligand densities may influence cell adhesion, spreading, and migration in different tissues and infection models (Bank et al., 1994; Palecek et al., 1997). For example, intravital imaging suggested that the morphologies of *Itgae*$^{-/-}$ T_{RM} and WT T_{RM} were equivalent in the skin following HSV infection (Zaid et al., 2017). In contrast, a recent study using a two-dimensional (2D) *in vitro* system demonstrated that $CD8^+$ T cells on an e-cadherin substrate displayed significantly more cell processes than cells plated on collagen IV. Rather, collagen IV-CD49a interaction promoted $CD8^+$ T cell migration *in vitro,* as well as in the trachea *in vivo* (Reilly et al., 2020). Although our data suggest that CD49a was not required for $CD8^+$ T cell migration into the epidermis, CD49a did regulate T_{RM} dendritic extensions in the skin *in vivo.* Future studies will examine how this affects T_{RM} migration within the epidermis.

Our results also suggest that CD49a augments T_{RM} cytokine secretion. We found that IFN-γ transcripts were increased in the skin of HSV-immune WT mice compared with *Itga1*$^{-/-}$ mice following local antigen challenge. Here, we demonstrated an increased fraction of WT OT-I compared with *Itga1*$^{-/-}$ OT-I T_{RM} produced IFN-γ following intradermal antigen challenge, suggesting that CD49a increases T_{RM} IFN-γ secretion *in vivo.* Whether CD49a acts as a costimulatory receptor or regulates $CD8^+$ T_{RM} migration/dendrite probing to increase antigen encounter *in vivo* will require additional studies. Previous studies suggest that CD103 restrains T cell motility, while CD49a facilitates migration (Reilly et al., 2020; Zaid et al., 2017). Our results suggest that CD49a and CD103 expression are differentially regulated by IL-12. Future studies will examine whether IL-12 might regulate adhesion receptor expression to coordinate T_{RM} behavior during the response to antigen challenge.

Finally, our data highlight a difference in the requirement of CD49a for $CD8^+$ T cell response during the acute versus memory phases of the immune response to HSV infection. During the primary response, *Itga1*$^{-/-}$ $CD8^+$ effector T cells accumulated within the skin and secreted IFN-γ upon *ex vivo* stimulation, suggesting that CD49a is dispensable for

effector $CD8^+$ T cell migration and response. Indeed, *Itga1*$^{-/-}$ $CD8^+$ effector T cells cleared replicating virus comparably to WT $CD8^+$ effector T cells during the primary response to HSV infection. In contrast, fewer *Itga1*$^{-/-}$ than WT $CD8^+$ T_{RM} persisted within the epidermis at memory time points, and they exhibited decreased effector function *in vivo* following cognate antigen challenge. Both reduced *Itga1*$^{-/-}$ $CD8^+$ T_{RM} persistence and decreased effector response to antigen challenge might contribute to impaired viral clearance by *Itga1*$^{-/-}$ $CD8^+$ T_{RM} in the memory phase.

In summary, CD49a serves multiple functions to promote $CD8^+$ T_{RM} memory response. Our findings suggest that CD49a is not required for the initial $CD8^+$ T cell response to HSV infection. However, CD49a promotes the persistence of T_{RM} within skin and enhances T_{RM} effector function upon cognate antigen challenge. Of note, however, CD49a also defines IFN-γ^+ $CD8^+$ T_{RM} within vitiligo lesions (Cheuk et al., 2017); it is possible that CD49a expression by $CD8^+$ T_{RM} may have detrimental effects in local cutaneous diseases.

Therefore, our studies define the functions of CD49a in promoting cutaneous $CD8^+$ T_{RM} persistence and response within a local skin infection site and may have implications for treatment of inflammatory diseases mediated by $CD49a^+$ $CD8^+$ T_{RM}.

STAR★METHODS

RESOURCE AVAILABILITY

Lead Contact—Further information and requests for resources and reagents should be directed to and will be fulfilled by the Lead Contact, Shannon Bromley (sbromley@mgh.harvard.edu).

Materials Availability—This study did not generate new unique reagents.

Data and Code Availability—This study did not generate/analyze datasets or code.

EXPERIMENTAL MODEL AND SUBJECT DETAILS

Itga1$^{-/-}$ mice were obtained from Dr. David Topham (University of Rochester) with permission from Biogen Idec. C57BL/6 mice, OT-I mice, and B6.SJL-$Ptprc^aPep3^b$/BoyJ (CD45.1) mice were obtained from Jackson Laboratories or Charles River Laboratories. *Itga1*$^{-/-}$ mice were crossed with OT-I mice to generate *Itga1*$^{-/-}$ OT-I mice. OT-I mice were crossed with CD45.1 mice to generate OT-I CD45.1 mice. All mice were maintained on the C57BL/6 background. Mice were housed and bred in a specific pathogen-free micro-isolator environment at Massachusetts General Hospital. Adult male and female mice ranging from 6-12 weeks old were used in experiments. Animal studies were approved and carried out according to the standards and guidelines set forth by the Institutional Care and Use Committee at Massachusetts General Hospital.

METHOD DETAILS

HSV Infections—HSV-1 KOS (Colgrove et al., 2016) was obtained from Dr. David Knipe (Harvard University). HSV-OVA (Mackay et al., 2013) was obtained from Dr. Thomas Gebhardt (University of Melbourne). Epicutaneous infection by scarification was done by

abrading a small area of skin near the top of the spleen using 150-grit sandpaper attached to the end of a pencil (Goel et al., 2002). An (~5 mm^2) area of skin was abraded with 20 strokes of the sandpaper. Then, 10^6 plaque-forming units (PFU) of HSV-1 KOS or HSV-OVA in 10 μL HBSS was applied to the abraded site, and mice were bandaged for 2 days as described (Goel et al., 2002; van Lint et al., 2004).

Isolation of cells from tissues—Blood (0.5 mL) was collected from mice by cardiac puncture. Red blood cells were then lysed by incubation with ACK lysis buffer (150 mM NH_4Cl, 10 mM $KHCO_3$, 0.1 mM Na_2EDTA). A 1 cm^2 piece of skin at the initial infection site was excised, scraped to remove fat, minced, and digested in 5 mL skin digestion buffer which consists of RPMI containing 1% FBS, 10 mM HEPES, 0.4 mg/mL Liberase TM (Roche), 2.5 mg/mL hyaluronidase (Sigma), and 0.4 mg/mL DNase I (Sigma) at 37°C for 45 minutes. Enzymes were quenched by addition of 15 μL 0.5 M EDTA, and digested skin was then dissociated using the Tumor Imp 01 setting on a GentleMacs (Miltenyi). The resulting cell suspension was filtered and washed through a 70 μm nylon filter. For isolation of cells from epidermis and dermis, the epidermis was affixed to a piece of opsite flexigrid tape (Smith and Nephew). The skin was then floated dermis side down on 5 mL HBSS containing 3 mg/mL dispase (GIBCO) at 37°C for 60 minutes, and dermis was physically separated from epidermis. Epidermis and dermis were minced, digested with Liberase TM as described above, but for 35 minutes. Draining brachial LNs and spleen were isolated, mushed through a filter, and red blood cells were lysed by incubation with RBC lysis buffer (Sigma).

Staining for flow cytometry—Isolated leukocytes were surface-stained with antibodies directed against CD3 (145-2C11), CD45 (30-F11), CD45.1 (A20), CD45.2 (104), CD8 (5H10), CD4 (GK1.5), CD44 (IM7), CD49a (Ha31/8), CD103 (2E7), CD69 (H1.2/F3), KLRG1 (2F1/KLRG1), CD62L (MEL-14) all from Biolegend, BD Biosciences, eBioscience, or ThermoFisher. For tetramer staining, leukocytes were incubated with TruStain FcX (Biolegend) and surface stained for CD8. After washing, cells were incubated with H-$2K^b$-HSV/gB tetramer (NIH tetramer core facility) for 25 minutes at 37°C. Then, cells were washed and stained with antibodies directed against other cell surface markers. Cell viability was determined by staining with fixable viability dye eFluor 506 or eFluor 780 (eBioscience). For granzyme B staining, cells were surface stained, fixed and permeabilized with BD Cytofix/Cytoperm Kit (BD Bioscences), and then stained for granzyme B (GB11). The stained samples were acquired with LSRII, Fortessa X20 (BD), or CytoFlex (Beckman Coulter) flow cytometers and analyzed with FlowJo software (TreeStar). Cell numbers were determined using CountBright Absolute counting beads (Invitrogen) as described (Moon et al., 2009).

Standard intracellular cytokine analysis—Spleen and skin cell populations were cultured in 96-well round-bottom plates at 10^6 cells per well in complete CR10 media (RPMI, 10% FBS, 10 mM HEPES, 2 mM L-glutamine, 50 μM β-mercaptoethanol, 100 U/mL penicillin, 100 mg/mL streptomycin, and 0.1 mM non-essential amino acids). 10^6 irradiated splenocytes isolated from naive, congenic C57BL/6 mice were added to the wells with or without 10 μM of the HSV-1 gB498-505 peptide and 1 μg/mL anti-CD28 antibody.

10 μg/mL brefeldin A was added to the wells at the start of culture. After a 4 hour incubation at 37°C, cells were placed on ice, washed and stained with antibodies directed against CD3, CD8, CD45.1, CD45.2, CD44 and fixable viability dye. Cells were fixed and permeabilized using Fix and Perm media A and B (Thermo Fisher) and stained intracellularly with anti-IFN-γ (XMG1.2).

Adoptive transfer of transgenic CD8⁺ T cells—$CD8^+$ T cells were isolated from *Itga1*$^{-/-}$ OT-I or WT OT-I transgenic mice by negative selection (Miltenyi). Then, 5×10^4 $CD8^+$ T cells in 200 μL PBS were adoptively transferred i.v. into congenic recipient mice. *In vitro*-activated $CD8^+$ OT-I T cells were generated by activating splenocytes from OT-I transgenic mice with peptide-pulsed splenocytes. Briefly, 5×10^6 irradiated C57BL/6 splenocytes were pulsed with 1 ug/mL OVA (257-264) for 1 hour at 37°C. Then, 5×10^6 OT-I splenocytes were cultured with the OVA- pulsed splenocytes in 40 mL CR10 media. After 2 days, cultures were split daily with fresh CR10 media containing 7.5 ng/mL recombinant IL-2 (Peprotech). After 5 days of culture, 10^6 OT-I T cells in PBS were injected intravenously or intradermally into the flank of recipient congenic mice as described (Mackay et al., 2013).

Viral titers—A 1 cm^2 piece of skin at the primary infection site was removed from mice, minced and placed in 1 mL of DMEM (Life Technologies). Samples were frozen in a dry ice / ethanol bath and kept at −80°C until use. The presence of infectious virus in tissue samples was determined using p.f.u. assays on confluent Vero cell monolayers in 24-well plates (Blaho et al., 2005). Samples were thawed and homogenized using the GentleMACS homogenizer (Miltenyi) RNA_01 program, and 10-fold serial dilutions were then tested for plaque formation to determine viral titer in the original tissue sample. After two days, cell monolayers were stained with crystal violet staining solution (0.5% crystal violet in 20% ethanol) to visualize plaques.

Confocal immunofluorescence and analysis—To compare the morphology of WT and *Itga1*$^{-/-}$ $CD8^+$ T_{RM}, a 1 cm^2 piece of skin from the initial infection site was harvested, scraped of fat, and fixed at 4°C for 1 hour in PLP buffer (0.2 M NaH_2PO_4, 0.2M Na_2HPO_4, 0.2 M I-lysine and 0.1 M sodium periodate in 2% paraformaldehyde). The skin was blocked (PBS, 2% BSA, 0.5% normal serum block (Biolegend), 0.2% TruStain FcX (Biolegend) in PBS) for 2 hours at room temperature. Then, the skin was stained overnight with a 1:100 dilution of CD8β-PE (YTS156.7.7; Biolegend) at 4°C, followed by washing with PBS 0.1% Tween 20. Finally, the skin was counterstained with 0.1 μg/mL Hoescht solution to detect nuclei. Images were acquired with a confocal microscope (Carl Zeiss Microimaging) using a 40x objective. Z stack images through the skin whole-mounts were acquired with 1.2 μm intervals. Epidermis and dermis was identified based on autofluorescence at 633 nm. Image Processing was performed using FIJI software. Circularity measurements were performed in FIJI on maximum intensity projections that were first thresholded, dilated, closed, fill holes and eroded.

For analysis of γδ T cell and $CD8^+$ T_{RM} numbers and localization within the skin, a 1 cm^2 piece of skin from the initial infection site was harvested, scraped of fat, embedded in optimum cutting temperature (OCT) compound (Tissue-Tek), frozen on dry ice, 10 μm

sections were cut, and slides were dried for 1 hour at 37°C. Sections were fixed in ice-cold 1:1 acetone:methanol for 10 minutes, washed in PBS, and blocked for 1 hour at room temperature. Endogenous biotin was blocked using a biotin/streptavidin blocking kit (Vector laboratories). Sections were then incubated with biotinylated anti-CD45.2 antibody (1:50) for 1 hour at room temperature. Sections were washed with PBS 0.1% tween and then incubated with anti-CD8β-PE (1:100), anti-γδ TCR-AF488 (1:100), and SA-AF647 (1:100) for 1 hour at room temperature. Next, sections were washed with PBS 0.1% tween, counterstained with Hoescht, and mounted using Prolong Diamond. Images along the entire length of the skin sections were acquired with a confocal microscope (Carl Zeiss Microimaging) using a 20x objective and processed using FIJI software. $CD8^+$ T cells and γδ T cells were counted manually, and the density of cells was determined by extrapolating the number of cells imaged in the skin surface section (10 μm thick x measured length of epithelium in the field of view) to the number of cells per cm^2 skin as described (Mani et al., 2019). Nonconsecutive sections were analyzed.

***In vitro* cytokine stimulation assays—**Spleens were harvested from C57BL/6 mice, single-cell suspensions were prepared, and T cells were activated in culture with 1 μg/mL anti-CD3 and 1 μg/mL anti-CD28. Cells were split 1:2 with fresh media containing 7.5 ng/mL recombinant IL-2 daily starting 2 days after initial culture. After 5 days, the activated T cells were plated at 2×10^5 cells/well in 200 μL media containing mouse IL-7 at 10 ng/mL in 96-well U-bottomed plates. Where indicated, cultures were supplemented with the following cytokines (all from Peprotech): human TGF-β1 at 10 ng/mL, mouse IL-1 at 100 ng/mL, mouse IL-6 at 100 ng/mL, mouse IL-12 at 10 ng/mL, mouse IL-33 at 100 ng/mL, mouse TNF-α at 125 ng/mL, mouse IFN-γ at 10 ng/mL. Cells were then incubated for 72 hours before staining for flow cytometric analysis.

Antigen-independent generation of $CD8^+$ T_{RM} and recall response—To induce $CD8^+$ T_{RM} cells, 5×10^4 WT- or *Itga1*$^{-/-}$ $CD8^+$ OT-I T cells in 200 μL PBS were adoptively transferred i.v. into recipient mice. Recipient mice were then injected intradermally twice (separated by three days) with 3 μg of the plasmid, pODCAGGS (Mani et al., 2019) which encodes full length chicken ovalbumin, kindly provided by T. Mempel. At least 28 d after DNA vaccination, mice were injected i.p. with 500 μg anti-CD4 (GK1.5; Biolegend) and 300 μg anti-CD8 (clone YTS169.4; BioXCell) antibodies to deplete circulating T cells. After 4 d, mice were bled and stained for CD4 and CD8 to confirm T cell depletion. Then, mice were infected with 10^6 pfu HSV-OVA at the site of DNA vaccination. After 4 d, a 1 cm^2 piece of skin surrounding the infection site was isolated, minced and placed in 1 mL of DMEM (Life Technologies) for determination of viral titers by plaque assay.

Depletion of circulating $CD8^+$ T cells and peptide challenge—30 d after HSV-1 KOS infection, mice were injected i.p. with 300 μg anti-CD8 antibody (clone YTS169.4; BioXCell) in PBS. 4 d after anti-CD8 antibody injection, mice were bled, and blood stained for CD8 to ensure depletion of circulating $CD8^+$ T cells. Mice whose circulating $CD8^+$ T cells were not depleted were excluded from the experiment. Then, mice were injected intradermally at the initial infection site with 3 μg HSV gB(498-505) peptide in 50 μL PBS

or with 3 μg OVA(257-264) peptide. 10 hours post-challenge, mice were injected intravenously with 500 μL of 0.5 mg/mL brefeldin-A in PBS as described (Liu and Whitton, 2005) for subsequent direct intracellular cytokine staining. After 6 hours, the skin was harvested for direct intracellular cytokine staining.

Direct intracellular cytokine staining—For direct intracellular cytokine staining, spleen and a 1 cm^2 piece of skin at the peptide challenge site were harvested and placed on ice. Skin was minced and digested in skin digestion buffer containing 10 μg/mL Brefeldin A as described above. Recovered leukocytes were then stained in buffer containing Brefeldin A with antibodies directed against CD3, CD8, CD45.1, CD45.2, CD44 and fixable viability dye. Cells were fixed and permeabilized using Fix and Perm media A and B (Thermo Fisher) and stained intracellularly with anti-IFN-γ (XMG1.2).

RNA isolation and Reverse transcription (RT)- Quantitative (q) PCR—10 hours after peptide challenge, a 1 cm^2 piece of skin at the initial infection site was isolated. Fat was removed, the skin was minced, snap frozen in liquid nitrogen, and stored at −80°C until use. Skin samples were homogenized in TRIzol (ThermoFisher) using the GentleMACS homogenizer (Miltenyi) RNA_02 program. Total RNA was isolated from the skin, and RT-qPCR was performed as described (Means et al., 2003) with the LightCycler 96 quantitative PCR system (Roche). Primer sequences used for qPCR included: *B2m* F-CCGAACATACTGAACTGCTACGTAA ; *B2m* R-CCCGTTCTTCAGCATTTGGA ; *Cxcl9* F-AATGCACGATGCTCCTGCA; *Cxcl9* R-AGGTCTTTGAGGGATTTGTAGTGG; *Cxcl10* F-GCCGTCATTTTCTGCCTCA; *Cxcl10* R-CGTCCTTGCGAGAGGGATC; *Ifng* F-AACGCTACACACTGCATCTTGG; *Ifng* R-GCCGTGGCAGTAACAGCC.

QUANTIFICATION AND STATISTICAL ANALYSIS

Data was assessed for normality using D'Agostino and Pearson test. Student's t tests or Mann–Whitney tests were used depending on whether data exhibited Gaussian distribution. All statistical analyses were done in Prism v7.0 or v8.0 (Graphpad), and for all analyses p values of less than 0.05 were considered significant as indicated by one or more asterisks (*). All experiments were performed at least two times, with similar results obtained each time.

Supplementary Material

Refer to Web version on PubMed Central for supplementary material.

ACKNOWLEDGMENTS

We would like to thank Dr. David Topham for providing *Itga1*$^{-/-}$ mice, Dr. David Knipe for providing HSV-KOS and advice on working with HSV, and Dr. Thomas Gebhardt for providing HSV-OVA. The following reagent was obtained through the NIH Tetramer Core Facility: H-2K(b) HSV-1 gB 498-505 SSIEFARL. The graphical abstract was produced using BioRender. This work was supported by NIH grant R01 AI121546 (to S.K.B.).

REFERENCES

Andreasen SØ, Thomsen AR, Koteliansky VE, Novobrantseva TI, Sprague AG, de Fougerolles AR, and Christensen JP. (2003). Expression and functional importance of collagen-binding integrins,

alpha 1 beta 1 and alpha 2 beta 1, on virus-activated T cells. J. Immunol 171, 2804–2811. [PubMed: 12960301]

Ariotti S, Beltman JB, Chodaczek G, Hoekstra ME, van Beek AE, Gomez-Eerland R, Ritsma L, van Rheenen J, Marée AFM, Zal T, et al. (2012). Tissue-resident memory CD8+ T cells continuously patrol skin epithelia to quickly recognize local antigen. Proc. Natl. Acad. Sci. U S A 109, 19739–19744. [PubMed: 23150545]

Ariotti S, Hogenbirk MA, Dijkgraaf FE, Visser LL, Hoekstra ME, Song J-Y, Jacobs H, Haanen JB, and Schumacher TN (2014). T cell memory. Skin-resident memory $CD8^+$ T cells trigger a state of tissue-wide pathogen alert. Science 346, 101–105. [PubMed: 25278612]

Bank I, Book M, and Ware R (1994). Functional role of VLA-1 (CD49A) in adhesion, cation-dependent spreading, and activation of cultured human T lymphocytes. Cell. Immunol. 156, 424–437. [PubMed: 8025956]

Bergsbaken T, Bevan MJ, and Fink PJ (2017). Local inflammatory cues regulate differentiation and persistence of $CD8^+$ tissue-resident memory T cells. Cell Rep 19, 114–124. [PubMed: 28380351]

Blaho JA, Morton ER, and Yedowitz JC (2005). Herpes simplex virus: propagation, quantification, and storage. Curr. Protoc. Microbiol Chapter 14, Unit 14E.1.

Casey KA, Fraser KA, Schenkel JM, Moran A, Abt MC, Beura LK, Lucas PJ, Artis D, Wherry EJ, Hogquist K, et al. (2012). Antigen-independent differentiation and maintenance of effector-like resident memory T cells in tissues. J. Immunol 188, 4866–4875. [PubMed: 22504644]

Chapman TJ, and Topham DJ (2010). Identification of a unique population of tissue-memory CD4+ T cells in the airways after influenza infection that is dependent on the integrin VLA-1. J. Immunol 184, 3841–3849. [PubMed: 20200271]

Cheuk S, Schlums H, Gallais Sérézal I, Martini E, Chiang SC, Marquardt N, Gibbs A, Detlofsson E, Introini A, Forkel M, et al. (2017). CD49a expression defines tissue-resident $CD8^+$ T cells poised for cytotoxic function in human skin. Immunity 46, 287–300. [PubMed: 28214226]

Colgrove RC, Liu X, Griffiths A, Raja P, Deluca NA, Newman RM, Coen DM, and Knipe DM (2016). History and genomic sequence analysis of the herpes simplex virus 1 KOS and KOS1.1 sub-strains. Virology 487, 215–221. [PubMed: 26547038]

Conrad C, Boyman O, Tonel G, Tun-Kyi A, Laggner U, de Fougerolles A, Kotelianski V, Gardner H, and Nestle FO (2007). Alpha1beta1 integrin is crucial for accumulation of epidermal T cells and the development of psoriasis. Nat. Med 13, 836–842. [PubMed: 17603494]

Dadi S, Chhangawala S, Whitlock BM, Franklin RA, Luo CT, Oh SA, Toure A, Pritykin Y, Huse M, Leslie CS, and Li MO (2016). Cancer immunosurveillance by tissue-resident innate lymphoid cells and innate-like T cells. Cell 164, 365–377. [PubMed: 26806130]

de Fougerolles AR, Sprague AG, Nickerson-Nutter CL, Chi-Rosso G, Rennert PD, Gardner H, Gotwals PJ, Lobb RR, and Koteliansky VE (2000). Regulation of inflammation by collagen-binding integrins alpha1beta1 and alpha2beta1 in models of hypersensitivity and arthritis. J. Clin. Invest 105, 721–729. [PubMed: 10727440]

Gardner H (2014). Integrin $\alpha 1\beta 1$. Adv. Exp. Med. Biol 819, 21–39. [PubMed: 25023165]

Gebhardt T, Wakim LM, Eidsmo L, Reading PC, Heath WR, and Carbone FR (2009). Memory T cells in nonlymphoid tissue that provide enhanced local immunity during infection with herpes simplex virus. Nat. Immunol 10, 524–530. [PubMed: 19305395]

Goel N, Docherty JJ, Fu MM, Zimmerman DH, and Rosenthal KS (2002). A modification of the epidermal scarification model of herpes simplex virus infection to achieve a reproducible and uniform progression of disease. J. Virol. Methods 106, 153–158. [PubMed: 12393145]

Goldstein I, Ben-Horin S, Li J, Bank I, Jiang H, and Chess L (2003). Expression of the alpha1beta1 integrin, VLA-1, marks a distinct subset of human CD4+ memory T cells. J. Clin. Invest 112, 1444–1454. [PubMed: 14597770]

Haddadi S, Thanthrige-Don N, Afkhami S, Khera A, Jeyanathan M, and Xing Z (2017). Expression and role of VLA-1 in resident memory CD8 T cell responses to respiratory mucosal viral-vectored immunization against tuberculosis. Sci. Rep 7, 9525. [PubMed: 28842633]

Hemler ME, Jacobson JG, Brenner MB, Mann D, and Strominger JL (1985). VLA-1: a T cell surface antigen which defines a novel late stage of human T cell activation. Eur. J. Immunol 15, 502–508. [PubMed: 2986987]

Jiang X, Clark RA, Liu L, Wagers AJ, Fuhlbrigge RC, and Kupper TS (2012). Skin infection generates non-migratory memory CD8+ T(RM) cells providing global skin immunity. Nature 483, 227–231. [PubMed: 22388819]

Klonowski KD, Williams KJ, Marzo AL, Blair DA, Lingenheld EG, and Lefrançois L (2004). Dynamics of blood-borne CD8 memory T cell migration in vivo. Immunity 20, 551–562. [PubMed: 15142524]

Liu F, and Whitton JL (2005). Cutting edge: re-evaluating the in vivo cytokine responses of CD8+ T cells during primary and secondary viral infections. J. Immunol 174, 5936–5940. [PubMed: 15879085]

Mackay LK, Stock AT, Ma JZ, Jones CM, Kent SJ, Mueller SN, Heath WR, Carbone FR, and Gebhardt T (2012). Long-lived epithelial immunity by tissue-resident memory T (TRM) cells in the absence of persisting local antigen presentation. Proc. Natl. Acad. Sci. U S A 109, 7037–7042. [PubMed: 22509047]

Mackay LK, Rahimpour A, Ma JZ, Collins N, Stock AT, Hafon M-L, Vega-Ramos J, Lauzurica P, Mueller SN, Stefanovic T, et al. (2013). The developmental pathway for CD103(+)CD8+ tissue-resident memory T cells of skin. Nat. Immunol 14, 1294–1301. [PubMed: 24162776]

Mackay LK, Minnich M, Kragten NAM, Liao Y, Nota B, Seillet C, Zaid A, Man K, Preston S, Freestone D, et al. (2016). Hobit and Blimp1 instruct a universal transcriptional program of tissue residency in lymphocytes. Science 352, 459–463. [PubMed: 27102484]

Mani V, Bromley SK, Äijó T, Mora-Buch R, Carrizosa E, Warner RD, Hamze M, Sen DR, Chasse AY, Lorant A, et al. (2019). Migratory DCs activate TGF-β to precondition naïve $CD8^+$ T cells for tissue-resident memory fate. Science 366, eaav5728. [PubMed: 31601741]

Manickan E, and Rouse BT (1995). Roles of different T-cell subsets in control of herpes simplex virus infection determined by using T-cell-deficient mouse-models. J. Virol 69, 8178–8179. [PubMed: 7494346]

Masopust D, Vezys V, Wherry EJ, Barber DL, and Ahmed R (2006). Cutting edge: gut microenvironment promotes differentiation of a unique memory CD8 T cell population. J. Immunol 176, 2079–2083. [PubMed: 16455963]

Masopust D, Choo D, Vezys V, Wherry EJ, Duraiswamy J, Akondy R, Wang J, Casey KA, Barber DL, Kawamura KS, et al. (2010). Dynamic T cell migration program provides resident memory within intestinal epithelium. J. Exp. Med 207, 553–564. [PubMed: 20156972]

Means TK, Hayashi F, Smith KD, Aderem A, and Luster AD (2003). The Toll-like receptor 5 stimulus bacterial flagellin induces maturation and chemokine production in human dendritic cells. J. Immunol 170, 5165–5175. [PubMed: 12734364]

Moon JJ, Chu HH, Hataye J, Pagán AJ, Pepper M, McLachlan JB, Zell T, and Jenkins MK (2009). Tracking epitope-specific T cells. Nat. Protoc 4, 565–581. [PubMed: 19373228]

Nash AA, Jayasuriya A, Phelan J, Cobbold SP, Waldmann H, and Prospero T (1987). Different roles for L3T4+ and Lyt 2+ T cell subsets in the control of an acute herpes simplex virus infection of the skin and nervous system. J. Gen. Virol 68, 825–833. [PubMed: 2950204]

Oja AE, Piet B, van der Zwan D, Blaauwgeers H, Mensink M, de Kivit S, Borst J, Nolte MA, van Lier RAW, Stark R, and Hombrink P (2018). Functional heterogeneity of $CD4^+$ tumor-infiltrating lymphocytes with a resident memory phenotype in NSCLC. Front. Immunol 9, 2654. [PubMed: 30505306]

Palecek SP, Loftus JC, Ginsberg MH, Lauffenburger DA, and Horwitz AF (1997). Integrin-ligand binding properties govern cell migration speed through cell-substratum adhesiveness. Nature 385, 537–540. [PubMed: 9020360]

Park SL, Zaid A, Hor JL, Christo SN, Prier JE, Davies B, Alexandre YO, Gregory JL, Russell TA, Gebhardt T, et al. (2018). Local proliferation maintains a stable pool of tissue-resident memory T cells after antiviral recall responses. Nat. Immunol 19, 183–191. [PubMed: 29311695]

Peng H, Jiang X, Chen Y, Sojka DK, Wei H, Gao X, Sun R, Yokoyama WM, and Tian Z (2013). Liver-resident NK cells confer adaptive immunity in skin-contact inflammation. J. Clin. Invest 123, 1444–1456. [PubMed: 23524967]

Ray SJ, Franki SN, Pierce RH, Dimitrova S, Koteliansky V, Sprague AG, Doherty PC, de Fougerolles AR, and Topham DJ (2004). The collagen binding alpha1beta1 integrin VLA-1 regulates CD8 T

cell-mediated immune protection against heterologous influenza infection. Immunity 20, 167–179. [PubMed: 14975239]

Reilly EC, Lambert Emo K, Buckley PM, Reilly NS, Smith I, Chaves FA, Yang H, Oakes PW, and Topham DJ (2020). TRM integrins CD103 and CD49a differentially support adherence and motility after resolution of influenza virus infection. Proc. Natl. Acad. Sci. U S A 117, 12306–12314. [PubMed: 32439709]

Schenkel JM, Fraser KA, Vezys V, and Masopust D (2013). Sensing and alarm function of resident memory $CD8^+$ T cells. Nat. Immunol 14, 509–513. [PubMed: 23542740]

Schenkel JM, Fraser KA, Beura LK, Pauken KE, Vezys V, and Masopust D (2014). T cell memory. Resident memory CD8 T cells trigger protective innate and adaptive immune responses. Science 346, 98–101. [PubMed: 25170049]

Schindelin J, Arganda-Carreras I, Frise E, Kaynig V, Longair M, Pietzsch T, Preibisch S, Rueden C, Saalfeld S, Schmid B, et al. (2012). Fiji: an open-source platform for biological-image analysis. Nat. Methods 9, 676–682. [PubMed: 22743772]

Teijaro JR, Turner D, Pham Q, Wherry EJ, Lefrancois L, and Farber DL (2011). Cutting edge: Tissue-retentive lung memory CD4 T cells mediate optimal protection to respiratory virus infection. J. Immunol 187, 5510–5514. [PubMed: 22058417]

van Lint A, Ayers M, Brooks AG, Coles RM, Heath WR, and Carbone FR (2004). Herpes simplex virus-specific CD8+ T cells can clear established lytic infections from skin and nerves and can partially limit the early spread of virus after cutaneous inoculation. J. Immunol 172, 392–397. [PubMed: 14688347]

Wakim LM, Woodward-Davis A, Liu R, Hu Y, Villadangos J, Smyth G, and Bevan MJ (2012). The molecular signature of tissue resident memory CD8 T cells isolated from the brain. J. Immunol 189, 3462–3471. [PubMed: 22922816]

Wang D, Yuan R, Feng Y, El-Asady R, Farber DL, Gress RE, Lucas PJ, and Hadley GA (2004). Regulation of CD103 expression by CD8+ T cells responding to renal allografts. J. Immunol 172, 214–221. [PubMed: 14688328]

Wu T, Hu Y, Lee Y-T, Bouchard KR, Benechet A, Khanna K, and Cauley LS (2014). Lung-resident memory CD8 T cells (TRM) are indispensable for optimal cross-protection against pulmonary virus infection. J. Leukoc. Biol 95, 215–224. [PubMed: 24006506]

Zaid A, Mackay LK, Rahimpour A, Braun A, Veldhoen M, Carbone FR, Manton JH, Heath WR, and Mueller SN (2014). Persistence of skin-resident memory T cells within an epidermal niche. Proc. Natl. Acad. Sci. U S A 111,5307–5312. [PubMed: 24706879]

Zaid A, Hor JL, Christo SN, Groom JR, Heath WR, Mackay LK, and Mueller SN (2017). Chemokine receptor-dependent control of skin tissue-resident memory T cell formation. J. Immunol 199, 2451–2459. [PubMed: 28855310]

Zhang N, and Bevan MJ (2013). Transforming growth factor-β signaling controls the formation and maintenance of gut-resident memory T cells by regulating migration and retention. Immunity 39, 687–696. [PubMed: 24076049]

Highlights

- IL-12 or TGF-β can induce CD49a expression by $CD8^+$ T cells
- CD49a is not required for $CD8^+$ T cell entry into or localization within the epidermis
- CD49a promotes $CD8^+$ T_{RM} persistence within the epidermis
- CD49a regulates T_{RM} dendritic morphology and response to antigen challenge

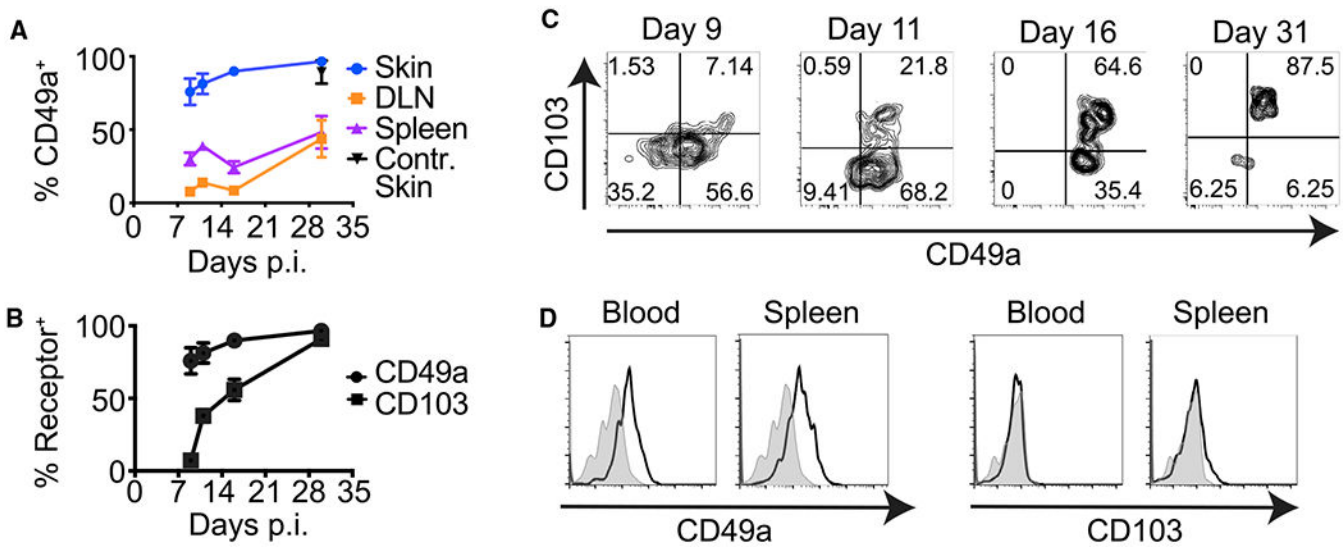

Figure 1. Differing Kinetics of CD49a and CD103 Expression by HSV-gB/K^{b} CD8^{+} T Cells

(A) CD49a expression by HSV-gB/K^{b} CD8^{+} T cells in the spleen, draining lymph node (DLN), initial skin infection site, and contralateral (Contr.) skin at the indicated times post-HSV KOS infection (p.i.). Error bars denote SEM.

(B) Frequencies of CD49a^{+} versus CD103^{+} HSV-gB/K^{b} CD8^{+} T cells in the skin at the indicated times post-infection. Error bars denote SEM.

(C) Representative flow cytometry plots demonstrating expression of CD49a and CD103 by cutaneous HSV-gB/K^{b} CD8^{+} T cells at the indicated times post-infection.

(D) Representative histograms showing frequencies of CD49a^{+} HSV-gB/K^{b} CD8^{+} T cells versus CD103^{+} HSV-gB/K^{b} CD8^{+} T cells in the DLN, blood, and spleen 7 days post-infection (gray shading, fluorescence minus one [FMO] control; black line, stained cells). Data are pooled from two experiments with six mice per time point (A and B) or are representative of two experiments with six mice per time point (C and D).

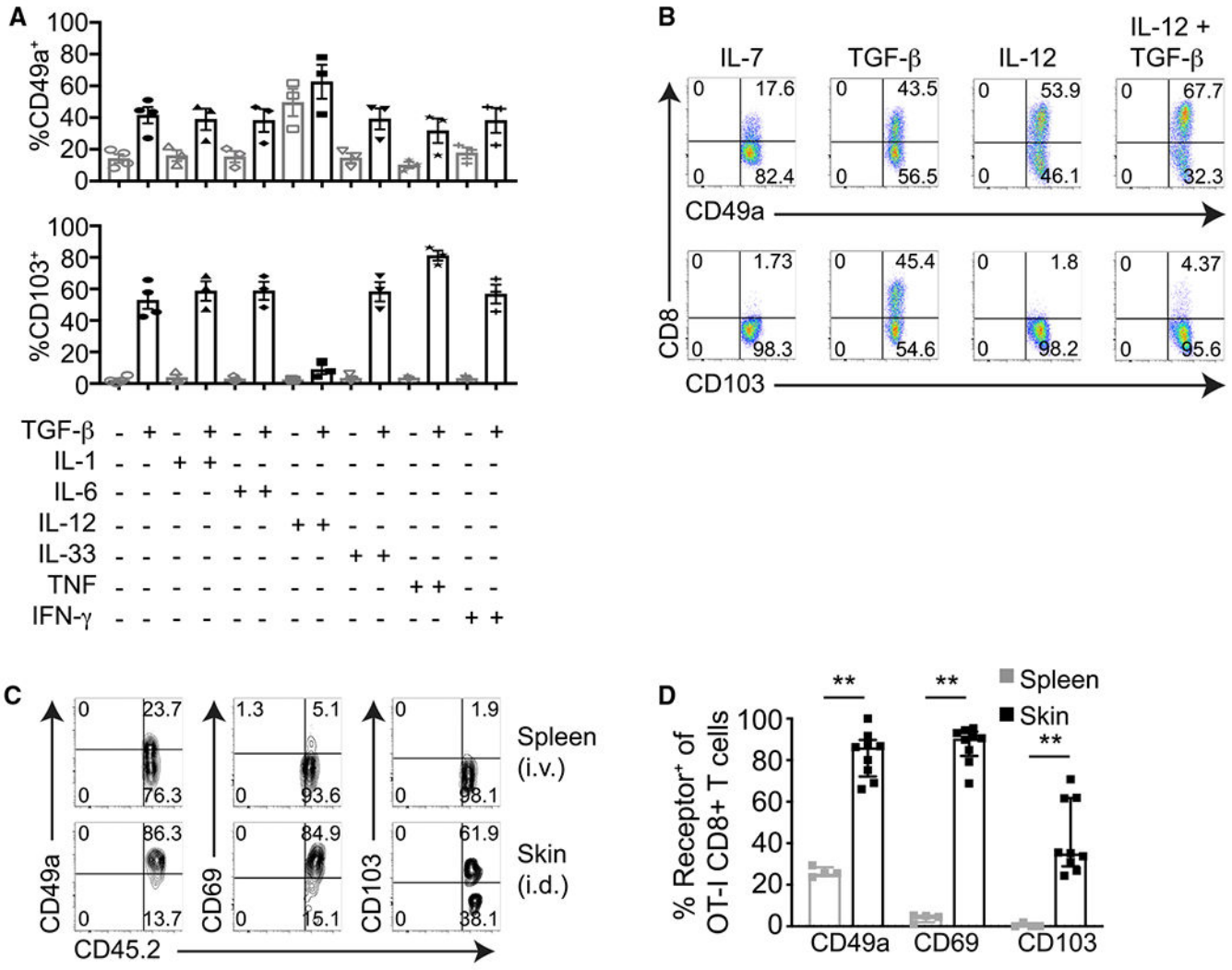

Figure 2. Differential Regulation of CD49a and CD103 Expression in CD8$^+$ T Cells by Cytokines

(A and B) Day 5 *in vitro* anti-CD3- and anti-CD28-activated CD8$^+$ T cells were incubated for 3 days with the indicated cytokines and then examined for their expression of CD103 and CD49a by flow cytometry. (A) Frequencies of CD49a$^+$ or CD103$^+$ CD8$^+$ T cells after *in vitro* culture with cytokines. Error bars denote SEM. (B) Representative flow cytometry plots demonstrating CD49a or CD103 expression by CD8$^+$ T cells after *in vitro* culture with cytokines.

(C and D) Day 5 *in vitro*-activated CD8$^+$ CD45.2$^+$ OT-I T cells were injected intravenously (i.v.) or intradermally (i.d.) into CD45.1$^+$ recipient mice. (C) Flow cytometry plots of CD49a, CD69, and CD103 expression by OT-I T cells recovered from the spleen 9 days after i.v. transfer and from the skin 9 days after i.d. transfer (gated on CD8$^+$ CD45.2$^+$ T cells). (D) Frequencies of CD49a$^+$, CD103$^+$, or CD69$^+$ CD8$^+$ OT-I T cells recovered from the spleen and skin 9 days post-transfer. **p = 0.0028, two-tailed Mann-Whitney test. Median, IQR.

Data are compiled from at least three experiments (A), are representative of at least three experiments (B), are representative of three experiments (C), or are pooled from three experiments with nine i.d. mice and four i.v. mice total (D).

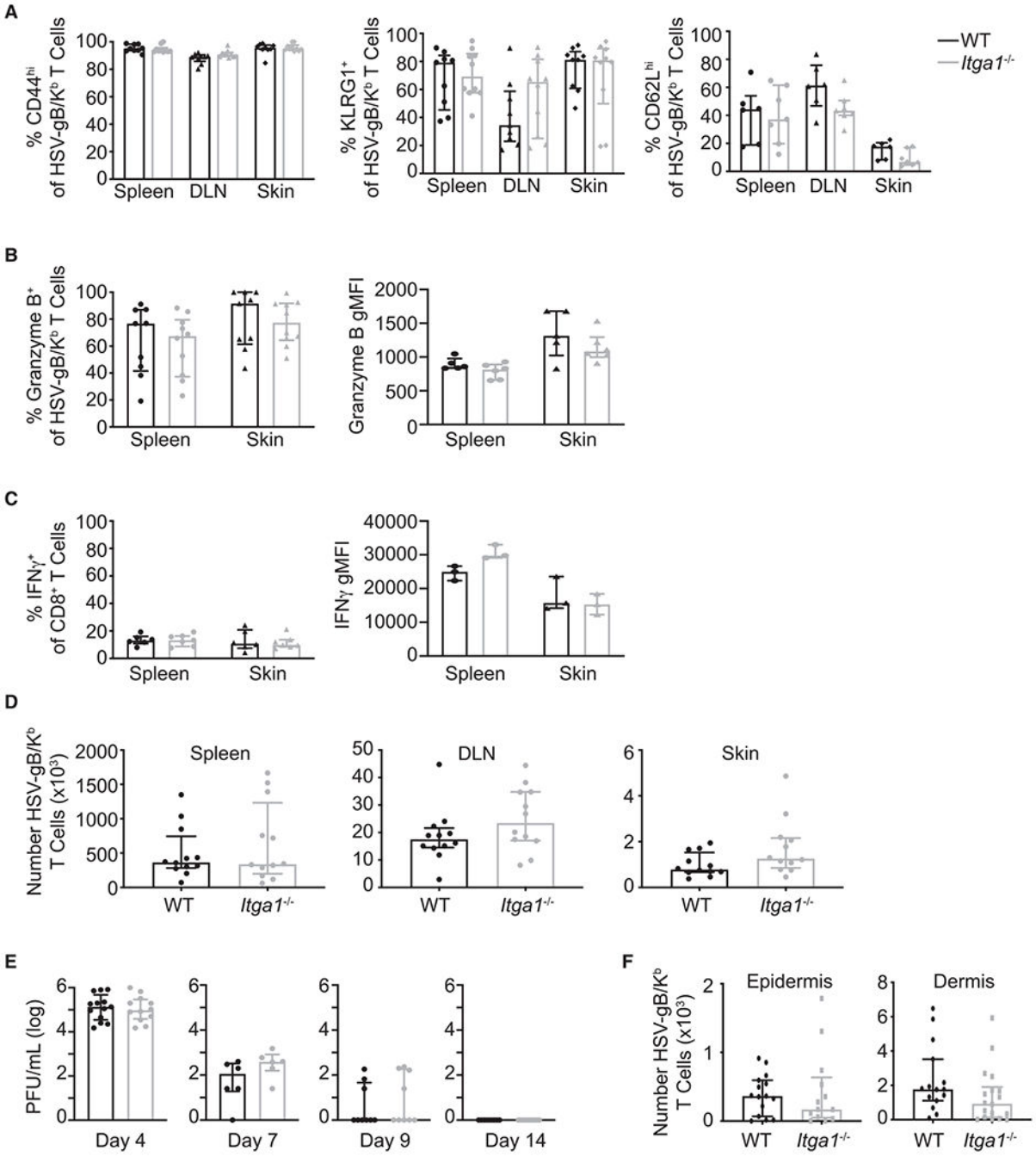

Figure 3. *Itga1*$^{-/-}$ HSV-gB/K^{b} CD8^{+} T Cells Are Activated, Enter into the Skin, and Clear Replicating HSV

WT and *Itga1*$^{-/-}$ mice were infected with HSV-KOS.

(A and B) WT and *Itga1*$^{-/-}$ HSV-gB/K^{b} CD8^{+} T cells differentiate comparably following HSV infection. (A) Proportion of HSV-gB/K^{b} CD8^{+} T cells expressing CD44, KLRG1, and CD62L in spleen, DLN, and skin 7 days post-infection. Median, IQR. (B) Left panel: frequency of HSV-gB/K^{b} CD8^{+} T cells expressing granzyme B^{+} in spleen and skin 7 days post-infection. Right panel: granzyme B geometric mean fluorescence intensity gated on CD44^{hi} HSV-gB/K^{b} CD8^{+} granzyme B^{+} T cells. Median, IQR.

(C) Left panel: frequency of IFN-γ^+ among total $CD8^+$ T cells after *in vitro* re-stimulation of day 9 skin cells or splenocytes with gB(498–505) peptide. Right panel: IFN-γ geometric mean fluorescence intensity gated on $CD44^{hi}$ HSV-gB/K^b $CD8^+$ IFN-γ^+ T cells. Median, IQR.

(D) HSV-gB/K^b $CD8^+$ T cells enter comparably into HSV-infected skin of WT and *Itga1*$^{-/-}$ mice. Numbers of HSV-gB/K^b T cells recovered from the spleen, DLN, and skin of WT versus *Itga1*$^{-/-}$ mice 7 days post-infection. Median, IQR.

(E) Both WT and *Itga1*$^{-/-}$ mice clear replicating HSV. Skin HSV titers 4, 7, 9, and 14 days post-infection. Median, IQR.

(F) HSV-gB/K^b $CD8^+$ T cells migrate into the epidermis of HSV-infected skin of WT and *Itga1*$^{-/-}$ mice. Numbers of HSV-gB/K^b $CD8^+$ T cells recovered from the epidermis and dermis of WT versus *Itga1*$^{-/-}$ mice 14 days post-infection. Median, IQR.

Data are compiled from three experiments (A, B left panel, and E) or from two experiments (C left panel, D) or are representative of two experiments (B, C right panel). No significant differences between groups were observed using Mann-Whitney tests.

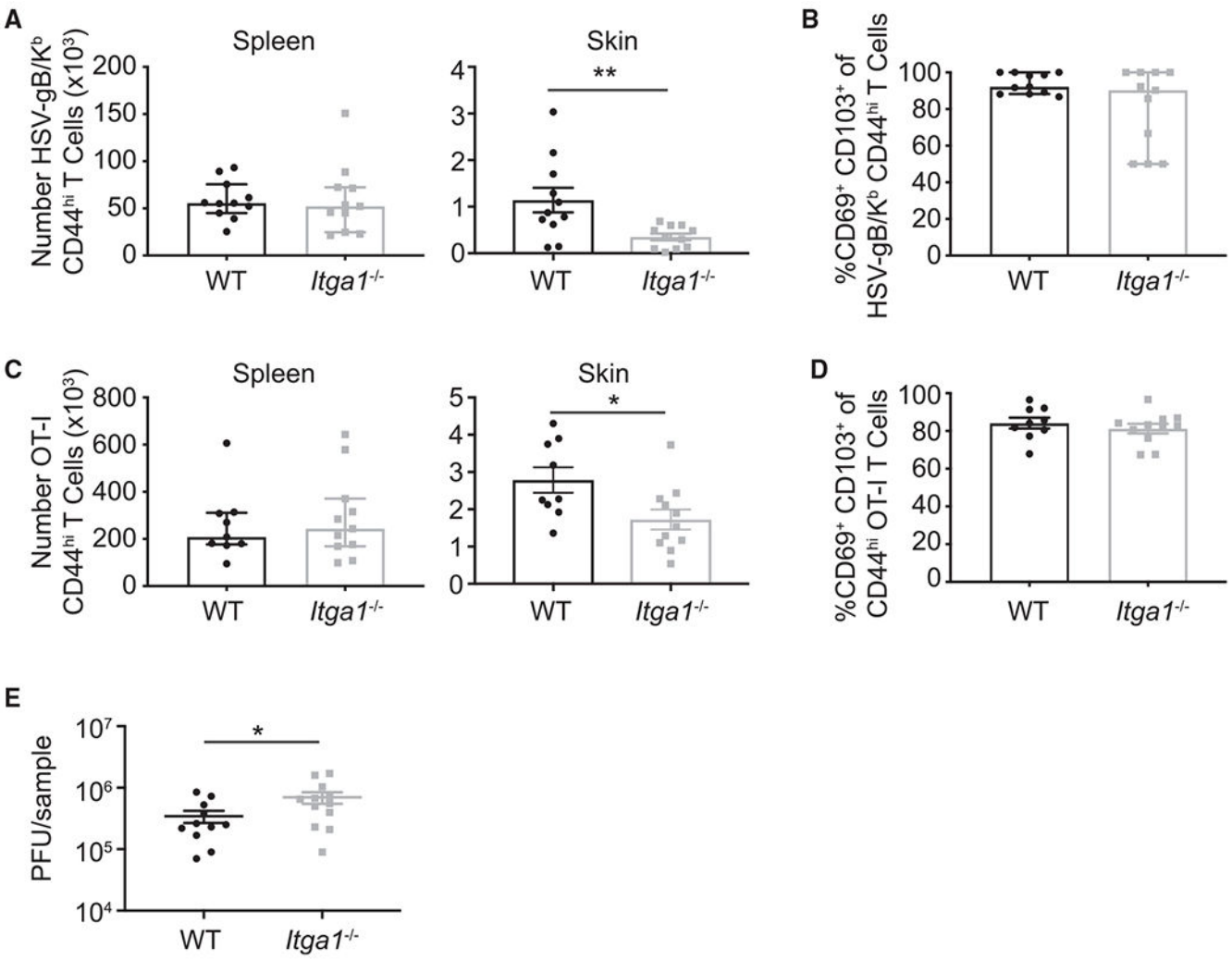

Figure 4. Decreased *Itga1*$^{-/-}$ HSV-gB/K^b CD8$^+$ T Cell Persistence

(A) Numbers of HSV-gB/K^b CD44^{hi} CD8$^+$ T cells recovered from the spleen and skin of WT versus *Itga1*$^{-/-}$ mice 35 days post-HSV-KOS-infection. **p = 0.0090, unpaired two-tailed t test. Error bars denote SEM.

(B) Frequency of CD69$^+$ CD103$^+$ HSV-gB/K^b CD44^{hi} CD8$^+$ T cells in the skin 35 days post-infection. No significant difference was observed using Mann-Whitney test. Median, IQR.

(C) WT OT-I CD8$^+$ T cells (5 × 10^4) or *Itga1*$^{-/-}$ OT-I CD8$^+$ T cells (5 × 10^4) were adoptively transferred into congenic recipient mice. Numbers of WT versus *Itga1*$^{-/-}$ CD49a-deficient OT-I CD44^{hi} T cells recovered from the spleen and skin 35 days post-HSV-OVA infection. *p = 0.0237, unpaired two-tailed Student's t test. Error bars denote SEM.

(D) Frequency of CD69$^+$ CD103$^+$ OT-I CD44^{hi} CD8$^+$ T cells in the skin 35 days post-infection. No significant difference was observed using unpaired two-tailed Student's t test. Error bars denote SEM. No significant difference was observed for spleen using Mann-Whitney tests. Median, IQR (A and C).

(E) WT OT-I $CD8^+$ T cells (5×10^4) or *Itga1*$^{-/-}$ OT-I $CD8^+$ T cells (5×10^4) were adoptively transferred into recipient mice, which were then injected twice intradermally with 3 μg OVA encoding plasmid. After 30 days, the injection site was infected with 10^6 plaque-forming units (PFU) HSV-OVA. Skin HSV titers 4 days post-challenge. $p = 0.0262$, unpaired one-tailed Student's t test. Error bars denote SEM.

Data are compiled from three experiments (A–D) or two experiments (E).

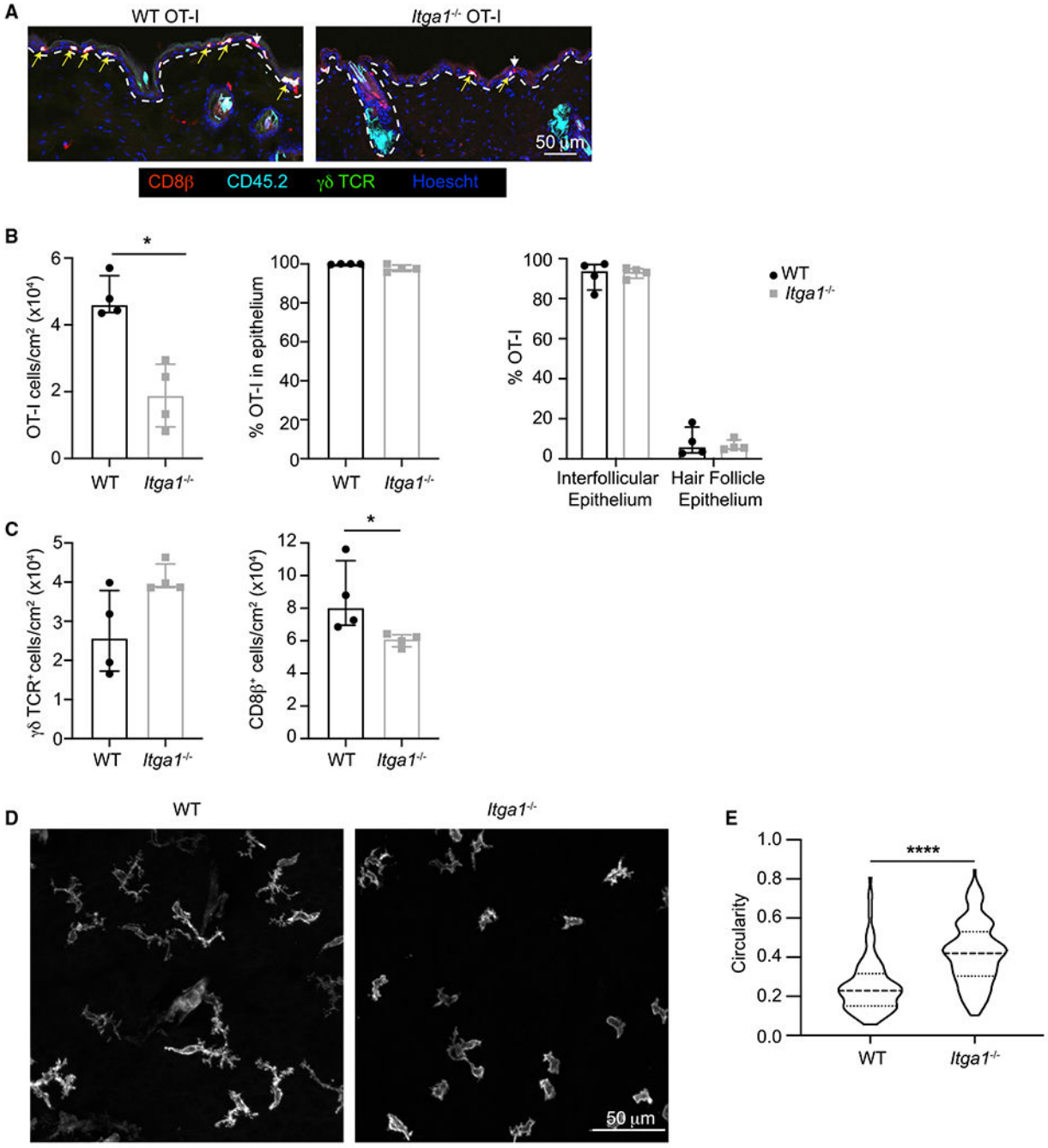

Figure 5. Comparison of WT and *Itga1*$^{-/-}$ Epidermal CD8^{+} T_{RM} Localization and Morphology

(A) WT CD45.2^{+} OT-I CD8^{+} T cells (5×10^4) or *Itga1*$^{-/-}$ CD45.2^{+} OT-I CD8^{+} T cells (5×10^4) were adoptively transferred into CD45.1^{+} recipient mice. Histological cross-sections of a 1 cm^2 area of flank skin surrounding the initial HSV infection sites. Yellow arrows indicate CD45.2^{+} OT-I T cells; white arrowheads indicate endogenous CD8^{+} T cells. Dashed lines indicate the dermal-epidermal border. Scale bar represents 50 um.

(B) Densities of WT and *Itga1*$^{-/-}$ OT-I T cells in the skin (left panel) and comparison of their localization within the epidermis (middle panel) and intrafollicular epithelium versus

hair follicle epithelium (right panel). Median, IQR. $p = 0.0286$, two-tailed Mann-Whitney test.

(C) Densities of γδ T cells (left panel) and $CD8b^+$ T cells (right panel) within the epidermis. Median, IQR. $p = 0.03$, two-tailed Mann-Whitney test.

(D) Representative images of epidermal $CD8b^+$ T cells in skin of HSV-infected WT or *Itga1*$^{-/-}$ mice at least 30 days post-infection. Scale bar represents 50 um.

(E) Circularity of epidermal $CD8b^+$ T cells in skin of HSV-infected WT or *Itga1*$^{-/-}$ mice at least 30 days post-infection. $p < 0.0001$, two-tailed Mann-Whitney test. Median, IQR.

Data are compiled from two experiments, with a total of six WT and six *Itga1*$^{-/-}$ mice.

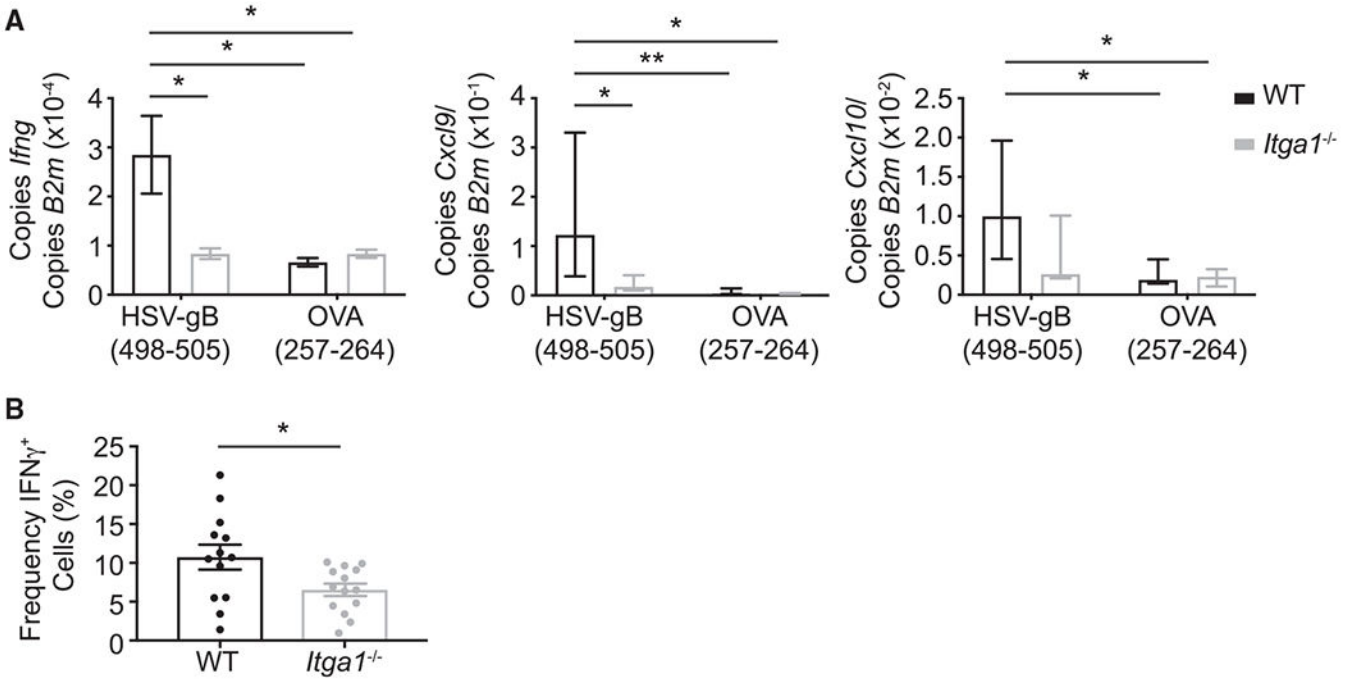

Figure 6. Reduced IFN-γ Secretion by *Itga1*$^{-/-}$ CD8^{+} T_{RM}

(A) WT or *Itga1*$^{-/-}$ mice were infected with HSV-KOS. Thirty-five days post-infection, the initial site of infection was injected intradermally with either gB or OVA peptide. *Ifng*, *Cxcl9*, and *Cxcl10* were measured using qRT-PCR from skin 10 h post-challenge. *Ifng*: *p = 0.0303, Student's t test, error bars denote SEM; *Cxcl9*: **p = 0.0052, Mann-Whitney test, median, IQR; *Cxcl10*: no significant difference using Mann-Whitney test, median, IQR. Data are compiled from three experiments, with a total of five to eight mice per condition. (B) WT OT-I CD8^{+} T cells (5×10^4) or *Itga1*$^{-/-}$ OT-I CD8^{+} T cells (5×10^4) were adoptively transferred into congenic recipient mice. Thirty-five days post-HSV-OVA infection, mice were injected locally with OVA peptide. Ten hours post-challenge, mice were injected i.v. with brefeldin A and sacrificed 6 h later. Cells recovered from the initial infection site were stained for IFN-γ. The frequency of IFN-γ^{+} cells among CD8^{+} CD44^{hi} CD103^{+} OT-I T cells is shown. *p = 0.0238, Student's t test. Error bars denote SEM. Data are compiled from three experiments.

KEY RESOURCES TABLE

REAGENT or RESOURCE	SOURCE	IDENTIFIER
Antibodies		
Ultra-Leaf Purified anti-mouse CD4 (GK1.5)	Biolegend	Cat# 100458; RRID AB_2810319
*In Vivo*Mab anti-mouse CD8α (YTS169.4)	BioXCell	Cat# BE0117; RRID AB_10950145
Ultra-Leaf Purified anti-mouse CD28 (37.51)	Biolegend	Cat# 102116; RRID AB_11147170
FITC anti-mouse CD3 (17A2)	Biolegend	Cat# 100204 RRID AB_312661
APC anti-mouse CD3 (17A2)	Biolegend	Cat# 100236 RRID AB_2561456
BD Horizon BUV395 anti-mouse CD3ε (145-2C11)	BD Biosciences	Cat# 563565 RRID AB_2738278
APC anti-mouse CD4 (GK1.5)	Biolegend	Cat# 100412 RRID AB_3126997
Alexa Fluor 700 anti-mouse CD8α (5H10)	ThermoFisher Scientific	Cat# MCD0829 RRID AB_10375174
PE anti-mouse CD8β (YTS156.7.7)	Biolegend	Cat# 126608 RRID AB_961298
PerCP/Cyanine5.5 anti-mouse/human CD44 (IM7)	Biolegend	Cat# 103032 RRID AB_2076204
APC/Cyanine7 anti-mouse/human CD44 (IM7)	Biolegend	Cat# 103028 RRID AB_830785
Brilliant Violet 605 anti-mouse CD45 (30-F11)	Biolegend	Cat# 103140 RRID AB_2562342
PE anti-mouse CD45.1 (A20)	Biolegend	Cat# 110708 RRID AB_313497
Biotin anti-mouse CD45.2 (104)	Biolegend	Cat# 109804 RRID AB_313441
FITC anti-mouse CD45.2 (104)	Biolegend	Cat# 109806 RRID AB_313443
Alexa Fluor 647 anti-rat/mouse CD49a (Ha31/8)	BD Biosciences	Cat# 562113 RRID AB_11153312
APC anti-mouse CD62L (MEL-14)	Biolegend	Cat# 104412 RRID AB_313099
PE/Cyanine7 anti-mouse CD69 (H1.2F3)	Biolegend	Cat# 104512 RRID AB_493564
Pacific Blue anti-mouse CD103 (2E7)	Biolegend	Cat# 121418 RRID AB_2128619
Alexa Fluor 488 anti-mouse TCR γ/δ (GL3)	Biolegend	Cat# 118128 RRID AB_2562771
Pacific Blue anti-human/mouse Granzyme B (GB11)	Biolegend	Cat# 515408 RRID AB_2562196
Brilliant Violet 421 anti-mouse IFN-γ (XMG1.2)	Biolegend	Cat# 505830 RRID AB_2563105
PerCP/Cyanine5.5 anti-mouse/human KLRG1 (MAFA) (2F1/KLRG1)	Biolegend	Cat# 138418 RRID AB_2563015
TruStain FcX (anti-mouse CD16/32) (93)	Biolegend	Cat# 101320 RRID AB_1574975)
Bacterial and Virus Strains		
HSV-KOS	Dr. David Knipe Harvard Medical School (Colgrove et al., 2016)	N/A
HSV-OVA	Dr. Thomas Gebhardt University of Melbourne (Mackay et al., 2013)	N/A
Chemicals, Peptides, and Recombinant Proteins		
OVA peptide (257-264) SIINFEKL	GenScript	Cat# RP10611
HSV-gB2 (498-505) SSIEFARL	GenScript	Cat# RP19992
Recombinant murine IL-1β	Peprotech	Cat# 211-11B
Recombinant murine IL-2	Peprotech	Cat# 212-12
Recombinant murine IL-6	Peprotech	Cat# 216-16
Recombinant murine IL-12 p70	Peprotech	Cat# 210-12

REAGENT or RESOURCE	SOURCE	IDENTIFIER
Recombinant murine IL-33	Peprotech	Cat# 210-33
Recombinant murine IFN-γ	Peprotech	Cat# 315-05
Recombinant human TGF-β1	Peprotech	Cat# 100-21
Recombinant murine TNF-α	Peprotech	Cat# 315-01A
eBioscience Fixable viability dye eFluor 506	ThermoFisher Scientific	Cat# 65-0866-18
eBioscience Fixable viability dye eFluor 780	ThermoFisher Scientific	Cat# 65-0865-14
BD Cytofix/Cytoperm Fixation/Permeabilization Solution Kit	BD Biosciences	Cat# 554715
PE-labeled H-2K^{b}-HSV/gB SSIEFARL	NIH tetramer core	N/A
Liberase TM Research Grade	Sigma Aldrich	Cat# 5401127001
DNase I grade II, from bovine	Sigma Aldrich	Cat# 10104159001
Brefeldin A	Sigma Aldrich	Cat# B6542
normal serum block	Biolegend	Cat# 927502
Crystal violet	Sigma Aldrich	Cat# C6158
OCT compound	Tissue-Tek	Cat# 4583
Tween20 molecular biology grade	Promega	Cat# H5151
Hoescht 33342, Trihydrochloride, Trihydrate	Thermo Fisher Scientific	Cat# H1399
Alexa Fluor 647 Streptavidin	Biolegend	Cat# 405237
TRIzol Reagent	Thermo Fisher Scientific	Cat# 15596018
FastStart Essential DNA Green Master	Roche	Cat# 06924204001
TaqMan Reverse Transcription Reagents	Thermo Fisher Scientific	Cat# N8080234
Critical Commercial Assays		
CD8+ T cell isolation kit, mouse	Miltenyi Biotec	Cat# 130-104-075
Countbright absolute counting beads	Thermo Fisher Scientific	Cat# C36950
Fix & Perm Cell Permeabilization kit	Thermo Fisher Scientific	Cat# GAS003
Streptavidin/Biotin Blocking kit	Vector Laboratories	Cat# SP-2002
Experimental Models: Cell Lines		
Vero Cells	Dr. Thorsten Mempel Massachusetts General Hospital	N/A
Experimental Models: Organisms/Strains		
Mouse: C57BL/6	The Jackson Laboratory	Cat# 027
Mouse: C57BL/6	Charles River Laboratoy	Cat# 000664
Mouse: OT-I. C57BL/6-Tg(TcraTcrb)1100Mjb/J	The Jackson Laboratory	Cat# 003831
Mouse: CD45.1. B6.SJL-Ptprc^{a} Pepc^{b}/BoyJ CD45.1	The Jackson Laboratory	Cat# 002014
Mouse: CD45.1. B6-Ly5.1/Cr	Charles River Laboratory	Cat# 564
Mouse: *Itga1*$^{-/-}$	(Ray et al., 2004)	N/A
Oligonucleotides		
B2m F-CCGAACATACTGAACTGCTACGTAA	This manuscript	N/A
B2m R-CCCGTTCTTCAGCATTTGGA	This manuscript	N/A
Cxcl9 F-AATGCACGATGCTCCTGCA	This manuscript	N/A

REAGENT or RESOURCE	SOURCE	IDENTIFIER
Cxcl9 R-AGGTCTTTGAGGGATTTGTAGTGG	This manuscript	N/A
Cxcl10 F-GCCGTCATTTTCTGCCTCA	This manuscript	N/A
Cxcl10 R-CGTCCTTGCGAGAGGGATC	This manuscript	N/A
Ifng F-AACGCTACACACTGCATCTTGG	This manuscript	N/A
Ifng R-GCCGTGGCAGTAACAGCC	This manuscript	N/A
Software and Algorithms		
ImageJ Fiji v1.0	(Schindelin et al., 2012)	https://imagej.net/Fiji
FlowJo v8, v10	TreeStar	https://www.flowjo.com/solutions/flowjo/downloads
Prism v7, v8	GraphPad	https://www.graphpad.com/scientific-software/prism/
CytExpert	Beckman Coulter	https://www.beckman.com/flow-cytometry/instruments/cytoflex/software
BD FACS DIVA 8	BD Biosciences	https://www.bdbiosciences.com/en-us/instruments/research-instruments/research-software/flow-cytometry-acquisition/facsdiva-software